

Copyright

by

Katrin E. Schmitt

2003

Optical neuronal guiding on the hypothalamic GnRH cell line GT1

by

Katrin E. Schmitt

THESIS

Presented to the Faculty of the Graduate School of
The University of Texas at Austin
in Partial Fulfillment
of the Requirements
for the Degree of

MASTER OF ARTS

THE UNIVERSITY OF TEXAS AT AUSTIN

August 2003

Optical neuronal guiding on the hypothalamic GnRH cell line GT1

APPROVED BY
SUPERVISING COMMITTEE:

Mark Raizen, Supervisor

Jason Shear

Dedicated to my family.

Acknowledgements

First of all, I want to thank my supervisor Prof. Mark Raizen for giving me the unique opportunity to work in his research group. It was a great experience and I learned a lot in this year. I appreciate the way he works together with his students, his unrestricted support and all his helpful discussions.

I also want to thank Samantha Moore and Florian Schreck, who introduced me to the project and worked together with me for the past year. Samantha, you taught me a lot in the beginning, all I know about cell culture I learned from you, and I am grateful you always helped me and supported me. I had a lot of fun in the lab.

Thanks also to Artem and Chuangwei for the nice atmosphere in the office, it was nice having you around. And of course there are all the other members of the Raizen group in the cold-atoms lab, who always helped me looking for optics parts and Florian.

Last but not least, I want to thank my parents and the rest of my family in Germany for their support during that year, which also contributed a lot to my having a pleasant stay here in Austin.

Optical neuronal guiding on the hypothalamic GnRH cell line GT1

Katrin Schmitt, M.A.

The University of Texas at Austin, 2003

Supervisor : Mark Raizen

This work describes experiments on optical neuronal guiding *in vitro* performed on the hypothalamic gonadotropin-releasing hormone (GnRH) cell line GT1. Briefly, a focused laser beam is set on the growing tip of the axon to induce further growth, making use of the dipole force the laser exerts on polarizable particles within the cell or in the cell membrane.

After a brief introduction to the idea of optical neuronal guiding and its first results, an outline of the cell line GT1 will be presented, followed by a comparison with the cell line NG108. The main part of this thesis presents the experimental setup, the experiments themselves and their results. The two final chapters discuss these results and give a theoretical approach.

Table of Contents

Acknowledgements	v
Abstract	vi
List of Tables	xi
List of Figures	xii
Chapter 1. Introduction	1
1.1 Why guide neurons?.....	1
1.2 First ideas.....	2
1.3 Optical guidance and its advantages.....	3
1.4 First results.....	6
Chapter 2. Background on neurons and the GT1 cell line	8
2.1 Basics about neurons.....	8
2.2 A special structure: the growth cone.....	11
2.3 The hypothalamus and its function within the nervous System.....	13
2.4 The hypothalamic cell line GT1.....	16
2.4.1 General characteristics.....	16

2.4.2	Differences between GT1-1 and GT1-7.....	21
2.5	GT1 versus NG108 and PC12.....	22
Chapter 3.	Experimental setup	24
3.1	Cell culture room.....	24
3.2	Setup of the optical elements and the visualization system....	27
3.2.1	Laser system.....	27
3.2.2	Optical elements on the beampath.....	33
3.2.3	The galvanometer system.....	35
3.2.4	Microscope setup.....	37
3.2.5	CCD camera.....	40
3.3	Sample stage.....	40
3.4	Design of the experimental dishes.....	41
3.5	The Neuron program.....	45
3.6	Preparation and setup of an experimental run.....	51
Chapter 4.	Results	53
4.1	Introduction.....	53
4.2	Induced morphological changes.....	55

Chapter 5. Discussion and theoretical considerations	71
5.1 Intrinsic mechanisms in GT1 cells.....	71
5.2 The correlation between action potentials and growth cone motility.....	75
5.3 Mechanosensitive ion channels.....	76
5.4 Involvement of calcium channels in the growth behavior of other types of cells.....	78
5.5 Considerations with regard to the GT1 cells.....	79
Chapter 6. Conclusions and Outlook	84
Appendices	87
Appendix A. List of chemicals	88
Appendix B. Cell culture procedures	90
B.1 Preparation of culture medium for GT1 cells.....	90
B.2 Preparation of PBS.....	91
B.3 Passaging.....	92
B.4 Plating on experimental dish.....	94
B.5 Thawing.....	95
B.6 Freezing.....	96

Appendix C. Program for avi-files	99
Appendix D. Protocol for cell culture people	102
Bibliography	104
Vita	111

List of Tables

2.1	Releasing and inhibiting hormones in the hypothalamus.....	15
2.2	Differences between GT1-1 and GT1-7 cells.....	22
4.1	Experimental results.....	60-62
A.1	List of chemicals.....	89

List of Figures

1.1	Neurons in the mammalian cortex.....	2
2.1	Single neurons in a drawing by Ramón y Cajal.....	8
2.2	The growth cone and its most important structures.....	12
2.3	Structure of the hypothalamus.....	13
2.4	Single GT1-1 neuron.....	16
2.5	GT1-1 cell in phase contrast image.....	17
3.1	pH-value of nutrient media dependent on CO₂-levels.....	25
3.2	Setup of the optics.....	28
3.3	Correlation between the absorption coefficient of water and different wavelengths in the near infrared.....	29
3.4	Power measurements with 0.5 attenuator.....	31
3.5	Power measurements with 0.8 attenuator.....	32
3.6	Laser beam path, schematic.....	33
3.7	Laser beam path in reality.....	34
3.8	Position of the laser spot in the focal plane.....	35
3.9	Beam path in the galvo system in reality.....	36

3.10	GT1-7 cells viewed through a standard light microscope.....	36
3.11	GT1-7 cells in phase contrast image.....	38
3.12	Microscope setup.....	39
3.13	Experimental dish on sample stage.....	41
3.14	Side view of the experimental dish.....	42
3.15	Side view and top view of the experimental dish.....	43
3.16	Bottom view of the experimental dish.....	44
3.17	Basic screen during a run.....	46
3.18	Details on the dialog box and the control buttons.....	48
3.19	Computer screen during an experiment.....	49
4.1	Schematic representation of neuronal growth cones.....	56
4.2	GT1-1 – induced morphological change.....	58
4.3	GT1-1 – growth cone rounding up.....	64
4.4	GT1-1 – cell with axon-like process.....	65
4.5	GT1-1 – single cell.....	66
4.6	GT1-1 – growth cone shape changes.....	67
4.7	GT1-1 – cell, reextending.....	68
4.8a+b	GT1-1 – cell, connections.....	69-70

Chapter 1

Introduction

1.1 Why guide neurons?

It has long been a fundamental objective to gain control over neuronal growth, and different approaches have been used in fields like neuroscience, cell biology and biophysics. More than a century ago, Ramón y Cajal discovered that the brain consists of an enormous number of discrete cells [1], which later were divided into two distinct groups: the neurons and the neuroglial cells. It was also Ramón y Cajal who first found that a neuron's axon makes contact to another neuron by a cleft – this cleft was eventually named “synapse” by Sherrington in 1897.

Since then, researchers have tried to understand more about the factors playing a role in neuronal growth and connections. The ability to control growing neurons is especially interesting for purposes like building artificial neuronal networks *in vitro*, i.e. cell culture, or nerve repair *in vivo*, i.e. in the living organism. Nerve regeneration is an important field where controlled neuronal growth can be used, because nerves in the central nervous system, which

comprises the brain and the spinal cord, do not regenerate naturally after damage, but have to be stimulated artificially. Therefore, a technique is desired which can accelerate neuronal growth and is as noninvasive as possible at the same time.



Figure 1.1: Neurons in the mammalian cortex.

This reproduction of a drawing of Ramón y Cajal shows a few neurons in the mammalian cortex. Only a few neurons contained in the sample of cortical tissue have been made visible by the staining procedure; the density of neurons is in reality much higher. Cell b is a nice example of a pyramidal cell with a triangularly shaped cell body. Dendrites, which leave the cell laterally and upwards, can be recognized by their rough surface. The axons are recognizable as thin, smooth lines which extend downwards with a few branches to the left and right. From Ramón y Cajal (1909).

1.2 First ideas

There have been many different attempts both *in vitro* and *in vivo* to influence and control neuronal growth. *In vivo*, for example, artificial guidance channels as implants have proven to be successful in nerve regeneration [2,3]. *In vitro*,

one possibility is to use artificial structures, such as silicon wafers [4], with a topographically changed surface to guide nerve growth. This altered surface can also be produced by a pattern in the substrate the cells adhere to [5,6] . Another group of researchers report the use of electrodes [7], where upon the application of an electric field *Xenopus* neurons tend to grow towards the cathode, but turn away from the anode. However, these methods have their disadvantages (as discussed in § 1.3).

1.3 Optical guidance and its advantages

Optical forces on microscopic objects were first reported by Ashkin in 1970 [8]. In his experiment, a single laser beam was sufficient to exert axial forces on a particle and push it through an aqueous chamber. With two opposed beams, the particle could be held stably trapped between the two beams. Also one tightly focused beam is sufficient to trap a particle. The fundamental principle for this phenomenon is that the stream of photons in a ray of light exerts “radiation pressure” on the particle as the light interacts with it. Conservation of momentum during the interaction demands that a force is generated on the object, which keeps it trapped in the beam. Intensity and coherence of the laser

beam guarantee a density of photons with uniformly directed momenta high enough for these applications.

The laser tweezers (single beam and two opposed beams) were further developed and improved for the microscopic manipulation of cells and organelles [9,10,11,12]. Here always the single beam conformation (either argon laser or near infrared light) was used by Ashkin *et al.* to demonstrate trapping of single cells, viruses and bacteria. Also non-biological particles, both in the Rayleigh and Mie-regimes, were observed to be trapped [9]. This was the first experimental observation of a single-beam gradient force particle trap.

Clearly, the laser tweezers have unique advantages for cell biology, like the delicate local control of forces, and therefore have found many applications since their invention. As one example, the study of the mechanical properties of neuronal growth cone membranes by tether formation with laser tweezers should be mentioned [13]. Coated beads, held by laser tweezers, attach to the membrane, and their mechanical properties can be studied through the extension of filopodia-like tethers with the beads.

About two years ago, it has been discovered by Ehrlicher *et al.* that it is possible to induce enhanced growth of the growth cone of a neuronal cell with a

focused laser beam spot [14]. Though the laser tweezer principle had crucial influence on this idea, in contrast to them weak optical forces are applied in this technique. A laser spot is placed on the leading edge of the growth cone and moved according to the response of the cell. This technique could be a new way to noninvasively control the natural process of neuronal growth.

One of the most obvious advantages is that, in comparison to other *in vitro*-techniques implementing guidance channels in the substrate, our technique does not sterically inhibit growth, which can lead to rupture of neurites because of tensions caused by these artificial pathways. Then, it does not rely on chemical treatments or substrate gradients on the surface. For the GT1, only laminin was used as coating to promote cell adhesion during cell culture (see Appendix B). Provided the experimental setup can be modified accordingly, also guiding in three dimensions is conceivable: the growth direction is only determined by the position of the laser focus, which could be adjusted and controlled to work in three dimensional space. Last, optical guiding is not restricted to a certain neuronal cell line, since it has already been shown to work for two neuronal cell lines. In fact, the technique seems applicable to other kinds of cells, on condition they are motile, i.e. moving. Here, human leukocytes and, as mentioned above, keratocytes have been guided successfully [M. Goegler,

private communication]. One reason that optical guiding seems to work on several different kinds of motile cells is that the dipole forces of the laser might directly influence actin polymerization, which is responsible for growth cone advance (discussed in § 2.2).

1.4 First results

Experiments were performed on the two cell lines PC12, a rat neuronal precursor cell line, and NG108, an immortalized mouse neuroblastoma rat glioma cell line.

It has been shown that in most cases the neuron responded with enhanced growth (about five to six times faster than naturally grown), or turns of the growth cone in another direction have been induced. Further experiments with the same experimental setup are being conducted on other kinds of motile cells like fibroblasts and keratocytes [15].

After the two above mentioned immortalized neuronal cell lines seemed to be good choices for our experiments, we were looking for another suitable immortalized neuronal cell line, which led us to start with the GT1 line. This is

an immortalized hypothalamic neuronal cell line established by Mellon and co-workers in 1990 [21].

Chapter 2

Background on neurons and the GT1 cell line

2.1 Basics about neurons

Neuronal cells are probably the most remarkable cells in both invertebrates and vertebrates based on the fact that they are capable of what no other cell type can do – build up a complex network of communication.

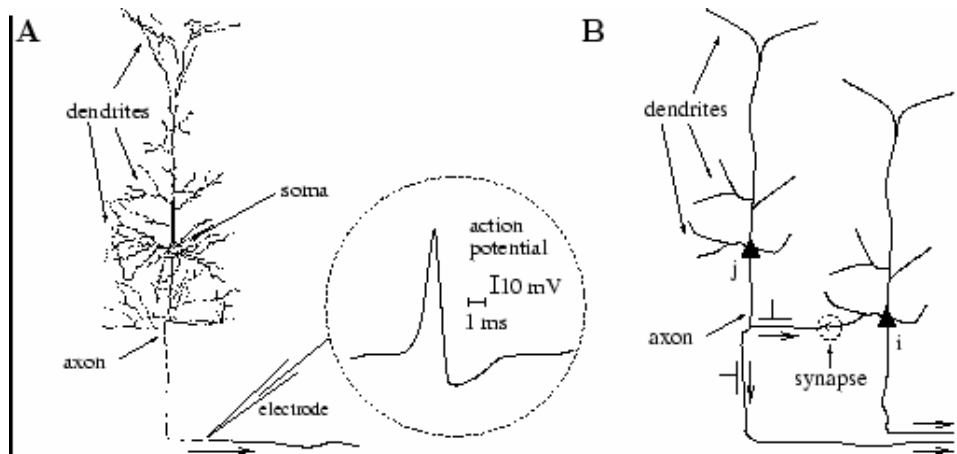


Fig 2.1: **A.** Single neuron in a drawing by Ramón y Cajal. Dendrite, soma and axon can be clearly distinguished. The inset shows an example of a neuronal action potential (schematic). The action potential is a short voltage pulse of 1-2 ms duration and an amplitude of about 100mV
B. Signal transmission from a presynaptic neuron *j* to a postsynaptic neuron *i*. The synapse is marked by the dashed circle. The axons at the lower right end lead to other neurons (schematic figure). From Ramón y Cajal, 1909.

Neurons are, in comparison to other biological cells, quite large cells with numerous, wide-spread branch-like projections (neurites) which can extend from the cell body only in the micrometer range, but sometimes become as long as one meter or more. Neurons elaborate an axon, the long neurite, and usually also shorter neurites called dendrites in order to make and receive connections. Neurite growth occurs at their advancing tips. They form a specialized structure called growth cones, where material transported from the cell body is incorporated into the cytoskeleton and the membrane. This structure is discussed in detail in § 2.2.

A very distinctive feature of neurons is the very large number of synapses they establish and maintain. In the human brain, for example, a typical nerve cell possesses tens of thousands of synapses, with many of them communicating at one time. Even more remarkable is the fact that these synapses are not stable, but exhibit plasticity; otherwise processes like learning or storing information (memory) would not be possible. One way to distinguish neurons is to divide them into the following three different types [16]: sensory neurons, which have special receptors to convert different stimuli (like light, touch, etc.) to electrical signals. These electrical signals are converted to chemical signals and sent to the next type, the so-called interneuron, where they are converted back to

electrical signals. After that, this information can be received by motor neurons, which then stimulate muscle cells, for example. The way electrical signals are transmitted along the axon is the action potential, which is evoked by opening and closing of specific ion-channels in the membrane. In the resting state, a voltage gradient (potential) of $\sim 70\text{mV}$ exists across the plasma membrane of the cell (inside of the cell counted negative to the outside). When an action potential occurs, the cell is depolarized to about $+40\text{mV}$ for a very short time period (milliseconds), and then returns to its original resting value (simplified model).

Another important fact for mammals is the distinction between central nervous system (CNS) and peripheral nervous system (PNS). In the central nervous system, which comprises brain and spinal cord, input is directly received from the senses and is processed. In the peripheral nervous system, which contains all other neuronal cells except those in brain and spinal cord, there are three sets of neurons: somatic and visceral sensory neurons, somatic motor neurons, and autonomic motor neurons (for further information about their functions see [16]).

2.2 A special structure: the growth cone

It was also Ramón y Cajal who first discovered the terminal enlargement of the axon in stained preparations of embryonic tissue and named it “growth cone”.

Attachment of growth cones occurs mainly at points of adhesion beneath the filopodia [18], and is essential for axonal growth. The growth of an axon in the nervous system follows a relatively precise pathway toward its target. *In vivo*, this can be influenced by different surfaces (noncellular components around the cell) or cell-cell communication via direct membrane contact. *In vitro*, neurons have been shown to prefer substrates to which they can strongly adhere. This substrate forms part of the extracellular matrix, containing proteins like fibronectin or, in our case, laminin. The attachment of cells to fibronectin or laminin is mediated by proteins called integrins, which can be found in the plasma membrane of neurons or other kinds of cells. Growth cones will also turn towards concentration gradients of some diffusible substances (chemotaxis), in particular Nerve Growth Factor (NGF).

The means by which additional membrane is added to the growth cone is not certain, but various models have already been proposed; one of them by Bray [20]. He suggests that most of the biosynthetic organelles are situated in the cell

body, and are transported as membrane precursors along the neurite to the growth cone. From here, they are transported to the tips of the filopodia, which are finger-like thin protrusions on the tip of the growth cone, by an interaction between a myosin-like protein on the vesicle surface and the actin in the microfilaments. Structures analogous to axonal growth cones can be found at the tips of developing dendrites.

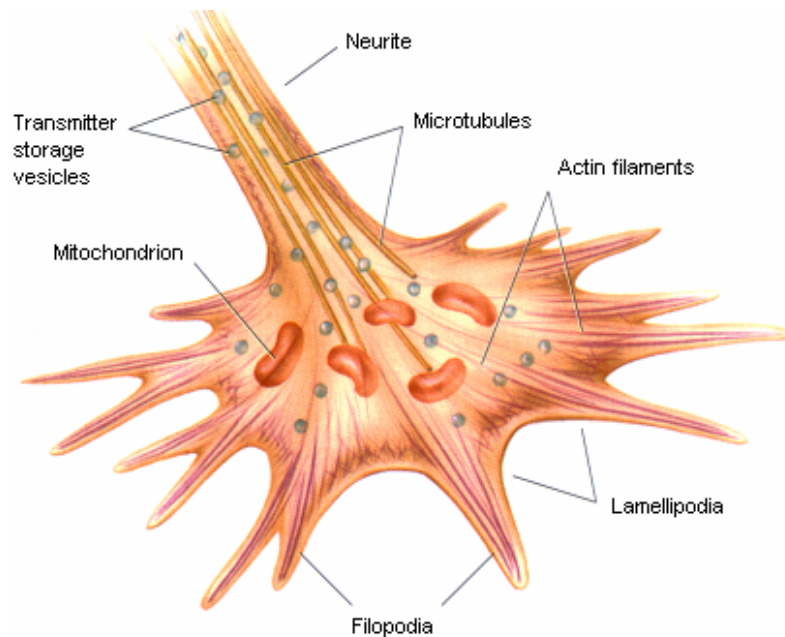


Fig 2.2: The growth cone and its most important structures; from ref. [19]

2.3 The hypothalamus and its function within the nervous system

The hypothalamus (lat. *corpora mamillaria*) is part of the diencephalon (interbrain) and controls all vegetative autonomous processes, i.e. it regulates homeostasis¹. Thalamus and hypothalamus are two anatomically and functionally distinct structures: the hypothalamus intercommunicates with the limbic system, whereas the thalamus is connected to the cortex.

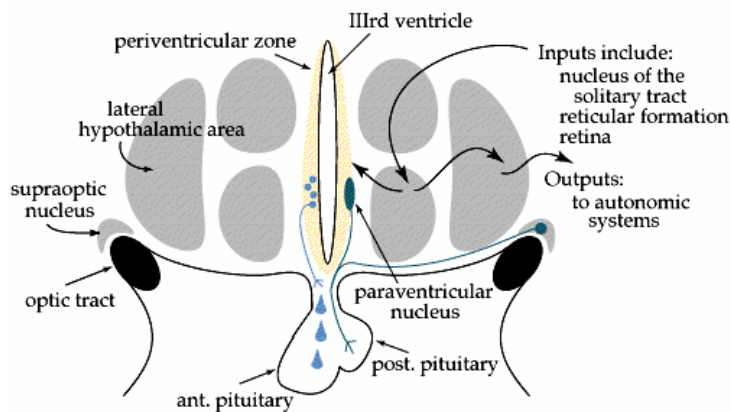


Fig 2.3:
Structure of the hypothalamus and its inputs and outputs in a coronal section; adapted from [17]

¹ Homeostasis is the maintenance of a constant internal environment (the immediate surroundings of cells) in response to changes in conditions of both the external and the internal environment: it works to maintain the organism's internal environment within its tolerance limits.

There are no direct afferent connections from the hypothalamus to the thalamus, only efferent connections from the hypothalamus to the unspecific thalamus.

These connections are used by the hypothalamus to control the higher sensory, motor and cognitive functions of thalamus and cortex. Different cortical areas have an indirect effect on the hypothalamus via the limbic system [17].

Because of its neurosecretory and anatomic connection to the pituitary gland, the hypothalamus is the center for control of many hormonal functions and the autonomic nervous system. In the hypothalamus, hormones are produced and stored, and their concentration is controlled (negative feedback). Factors like blood pressure, body temperature, fluid and electrolyte balance are held at a precise value; to achieve this task, the hypothalamus receives inputs about the actual state of these parameters, and initiates compensatory changes if necessary. We notice this need for changes when we feel hungry, or cold, for example. Via connections to the cortex, the hypothalamus also influences complex behavior patterns of addiction and consumption and evoke emotional reactions.

The following table summarizes different hormones produced by the hypothalamus and their effects.

Abbreviation	Name	Effect on
Releasing hormones		
TRH	Thyrotropin-RH	TSH (Thyrotropin)
LHRH	Luteinizing hormone-RH	FSH and LH
CRH	Corticotropin-RH	ACTH (adrenocortico- trophic hormone)
GHRH	Growth hormone-RH	GH
PRH	Prolactin-RH	Prolactin
Inhibiting hormones		
GHIH	Growth hormone-IH	GH
PIH	Prolactin-IH	Prolactin

Table 2.1: Releasing and inhibiting hormones in the hypothalamus. In red: LHRH, or GnRH (gonadotropin-releasing hormone), which is important in GT1 cells. Adapted from [18].

2.4 The hypothalamic cell line GT1

2.4.1 General characteristics

The GT1 is the first neuroendocrine clonal cell line derived from the central nervous system (CNS) and was developed by Mellon and co-workers [21]. All GT1 cells used in our experiments were a generous gift of Dr. Mellon.

Female mice carrying the hybrid GnRH-Tag gene, which expresses the SV40 T-antigen oncogene, developed forebrain tumors (post-migration of the GnRH neurons). From these tumors, clonal, differentiated, neurosecretory cell lines could be obtained. A pure cell population (GT1) was cloned by serial dilution into three subclones (GT1-1, GT1-3 and GT1-7). Though they are very similar in morphology, they differ in some characteristics, for example the growth rate (GT1-3 and GT1-7 double about every 36h, GT1-1 every 3-4 days).

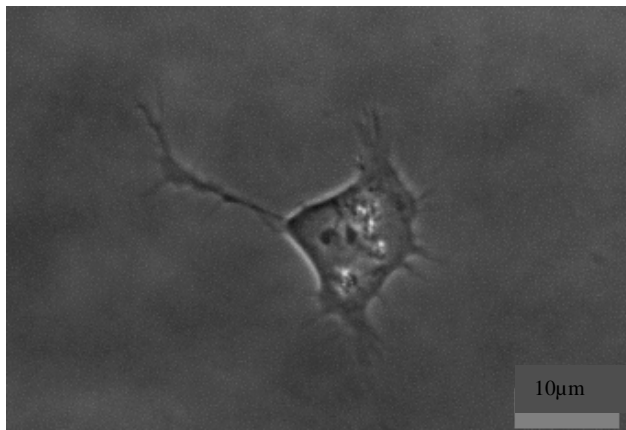


Fig 2.4: Single GT1-1 neuron plated on laminin after 48h in serum-free medium. Clearly visible are the extending axon and two nuclei in the cell body. Phase-contrast image

Further differences shall be discussed later in § 2.4.2. Common to all GT1 cells is that they extend neurites, express the endogenous mouse GnRH mRNA (messenger RNA), release GNRH/LHRH in response to depolarization, have fast regulating Na⁺ channels typical for neurons, and express neuronal, but not glial, cell markers [21]. In addition, they maintain several specific characteristics of neurosecretory cells at the ultrastructural level [23]: among them the Golgi apparatus, indented nuclei, rough endoplasmatic reticulum, secretory granules and regulation of secretion. Neuritic processes can be seen frequently extending from perikarya (cytoplasm surrounding the nucleus) containing neurosecretory granules or varicosities. When dividing, cells retract these neuritic processes, round up, and reextend them after division.

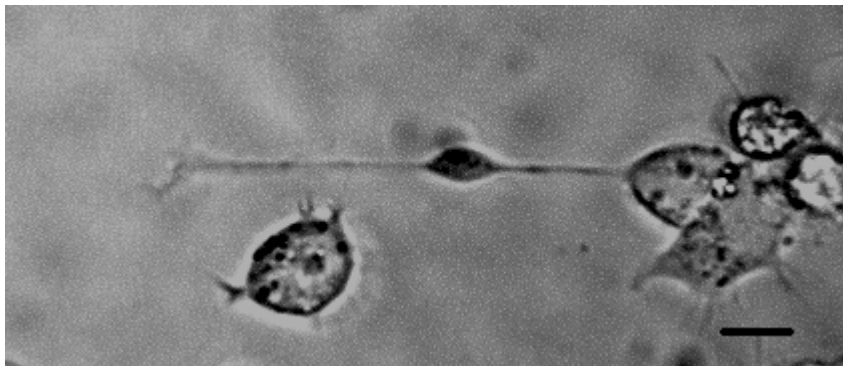


Fig. 2.5: GT1-1 cell in phase-contrast image, with a varicosity in the axon; these varicosities are a sign of mature, axon-like processes [23]. Scale bar, 10 μ m.

Since the development of immortalized² cell lines, the study of the mammalian GnRH system has been significantly advanced. GnRH/LHRH is a decapeptide which is secreted by the hypothalamus and then transported to the anterior pituitary gland, where it stimulates the release of FSH and LH (see also Table 2.1) [24]. The GT1 cells exhibit many physiological characteristics of GnRH neurons *in situ*, and are therefore very suitable for studies of GnRH single cells or neural networks. This is especially important since the mammalian reproductive system is regulated by complex interactions along the neuroendocrine axis, which comprises hypothalamus, anterior pituitary and gonadal signals. However, it has been difficult to investigate these regulatory mechanisms because of the anatomic topology of the GnRH system, where GnRH neurons are found in small number and scattered distribution and therefore are not easily accessible. Specifically, the cell bodies show this scattered distribution within the anterior hypothalamic region, whereas the nerve terminals (axons) converge on the median eminence. But, as shall be seen later, despite this scattered distribution, they communicate and transfer signals in a highly synchronized manner. Also, CNS tumors occur naturally only very

²Immortalized cells (mammalian) are capable of indefinite growth, i.e. the time cells need to divide is less than the rate at which they die. These special cells are either derived from tumor cells taken directly from an animal like in the case of the GT1s, or they are cultured cells that have undergone transformation

rarely and highly differentiated CNS cells like hypothalamic neurons are not easy to immortalize; previous attempts have met with little success [22].

The finding that LHRH is still prevalent in GT1 neurons is important because it demonstrates that the transformation by LHRH-Tag and the consequent immortalization does not disrupt the transcription and translation of the respective mRNAs.

Another common characteristic of all GT1 subclones is their episodic pattern of electrical activity [25], which is commonly associated with the pulsatile release of GnRH. Long-term recordings revealed that GT1-7 neurons fire spontaneous action potentials with a rate of 24.8 (+/- 1.3) min. These action potentials can be completely suppressed by the sodium channel blocker tetrodotoxin (TTX). The episodic changes seem to be part of the mechanism underlying the release of GnRH, because the firing frequencies of both action potentials and hormone release are consistent. Another paper focusing on the generation and synchronization of GnRH pulses reports a mean interpulse interval for secretion of GnRH of 25.8(+/- 1.5) min with a mean duration of 18.8 (+/- 1.4) min [26]. GnRH from GT1 neurons is also dependent on external Ca^{2+} [26,27]. When calcium is removed from the medium, pulsatile LHRH release is practically abolished [28]. Therefore, the cells express a variety of plasma membrane

channels which endow them with the ability to fire spontaneous action potentials (more about this topic in §); among them TTX-sensitive Na⁺ channels [21], three different types of outward K⁺ channels, a K⁺ inward rectifier [29, 30], and voltage-dependent L- and N-type Ca²⁺ channels [29, 31]. Despite all the advantages the development of the GT1 cells seem to have, one must keep some potential limitations in mind [32]. The signaling pathways and the kinds of receptors the immortalized cells express now might also be a result of the immortalization process and therefore not reflect traits found in differentiated GnRH neurons *in vivo*. The GT1 cells are also lacking input from any other afferent neurons and supporting glia cells, or other physiological circumstances like regulatory feedback loops usually present in the neuroendocrine axis, which might alter their pattern of expression. It is also unclear if the paracrine signals observed *in vitro* actually occur *in vivo*. They could also be only an artifact of the proximity of large numbers of GnRH cells in the chambers [26]. Therefore, certain patterns of behavior we can observe on GT1 cells *in vitro*, might not be valid in a cohesive neuroendocrine system like the one we carry in ourselves.

2.4.2 Differences between GT1-1 and GT1-7

Although they are derived from the same tumor and ultimately from the GT1 cells themselves, the different subclones (GT1-1, GT1-3 and GT1-7) show several differences among them [21, 23]. I will only present the GT1-1 and GT1-7 subclones, since these were the ones used in our experiments.

GT1-1 subclone	GT1-7 subclone
~ 10-50 μ m in size (cell body including neurites)	~20-80 μ m in size (cell body including neurites)
Less differentiated morphology: axons and dendrites not easily distinguishable	More differentiated: axons and dendrites clearly distinguishable and more pronounced
Tend to grow in clusters	Tend to form network-like growth pattern
More sensitive to plating procedures: require laminin for adhesion (see also Appendix A: cell culture procedures)	Attach very firmly even to non-coated coverslips or dishes. Require trypsin for detaching

Table 2.2: Differences between GT1-1 and GT1-7 cells

2.5 GT1 versus NG108 and PC12

The last paragraph introduced the most important features of the GT1 hypothalamic cell line. Now they shall be compared briefly with the cell lines NG108 and PC12, which were used in previous experiments [14].

Common to all three cell lines is that they are established cell lines and therefore immortal. Primary cell cultures are cells directly taken from a tissue source (animal) and grown in culture before subdivision and transfer to a subculture (cell strain). The problem with primary culture cells is that they have a finite life span and are unpredictable in their behavior, so experiments would be less reproducible with them. Established cell lines, however, have the ability of indefinite growth (immortality) and are therefore better suited for our experiments.

The probably most striking difference is that both PC12 cells and NG108 are PNS neurons, whereas GT1 are derived from neurons in the CNS (see § 2.1).

PC12 is a cell line derived from an adrenal gland tumor, or pheochromocytoma, of *Rattus norvegicus* rats [34]. They need NGF added to the culture medium to attach and fully differentiate, i.e. extend neurites.

The NG108 cell line was developed by Hamprecht in 1971 [35]. It is a somatic hybrid³ cell line which was formed by fusing mouse neuroblastoma⁴ with rat glioma⁵ cells in presence of inactivated Sendai virus. In comparison to PC12, they have less defined neural structures, but are more robust and easier to culture.

³Hybridization: combination of two different cell's characteristics, created by cell fusion often performed to create immortal cells

⁴neuroblastoma: malignant tumor derived from ganglion cells

⁵glioma: tumor derived from glial cells (supportive tissue of the brain)

Chapter 3

Experimental setup

3.1 Cell culture room

The cell culture room was built in Fall 2002 in our laboratory to provide a sterile environment for culturing the cells. Entry to and use of the cell culture room is restricted to authorized personnel only and in compliance with certain guidelines according to Biosafety Level 2 [36] (the protocol can be found in Appendix D). The room itself, which is entered through a pre-room, is equipped with a flow hood, two incubators, centrifuge, water bath, microscope and a shelf for storing cell culture supplies. Unless anyone is working inside, UV-light floods the whole room to reduce bacterial impact to a minimum.

We culture our cells in a humidified incubator at 37°C and 7.5% CO₂. The incubator (HERAcell CO₂ incubator, Heraeus [33]) has a copper inner casing, which reduces the possibility for bacterial or fungal infection in the humidification water or on the incubator walls. Copper ions do not become airborne and therefore pose no threat to cells incubated in flasks; however, they

do bond to contaminants such as bacteria and disrupt their metabolism.

Since we culture both NG108 and GT1 cells in the same incubator, we feed both cell lines with a mixture of Ham's F12 and DMEM (1:1) without HEPES buffer, and therefore set the value of the CO₂-level to 7.5%, based on the graph below. According to our experience, this seems to be a suitable value for both cell lines.

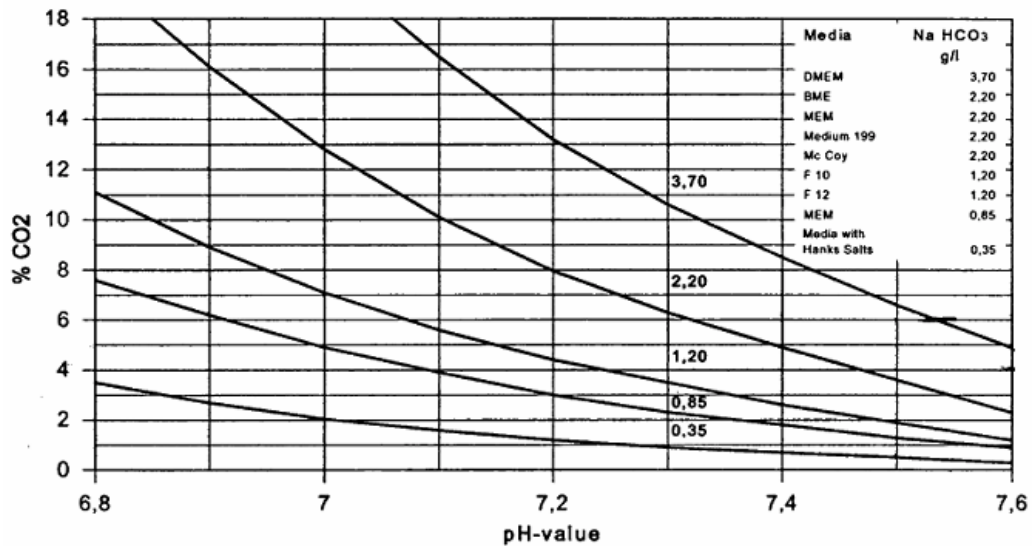


Fig 3.1: pH-value of nutrient media dependent on CO₂ levels.

The culture medium consists of 50% F12 (1.20-line) and 50% DMEM (3.70-line). When interpolating the two lines in the graph for a CO₂-value of 7.5%, we should get a pH-value of ~7.25, which is in the desired range. Measurements in the medium in the incubator with indicator paper show pH-values between 7.2 and 7.4. Figure adapted from [33].

The cells are grown in 75cm² cell culture flasks or petri dishes (Corning Inc.) in DMEM:F12 (1:1) supplemented with 10% fetal bovine serum (a complete list of chemical products used, their purpose and vendors, and cell culture procedures can be found in Appendices A and B, respectively). Cells attach to the surface of the flasks or dishes and are covered with 10ml medium, which has to be replaced daily or once in two days (depending on the confluency of the cells and therefore their consumption of nutrients in the medium). A slight change in the color of the medium from dark red to light red or orange or indicates that the medium needs to be replaced. This change in color is due to pH changes in the medium caused by cell waste, but does not indicate degradation of medium proteins such as L-glutamine. Currently we do not use penicillin in the culture medium, since the cells are only handled in a sterile environment within the culture room and thus the use of penicillin does not seem to be necessary.

The cell culture room is cleaned completely with 10% bleach once every two weeks to prevent contamination with bacteria or mold.

3.2 Setup of the optical elements and the visualization system

3.2.1 Laser system

We use two laser diodes (Blue Sky Research) and operate them in cw mode at a wavelength of 810nm. These diodes operate at the wavelength we need and in the optimal power range (output power 150mW max.). The spatial profile of the emitted beam is Gaussian, where the beam profile intensity is given by [37]:

$$I(r) = I_0 \exp\left[-\frac{2r^2}{\omega_0^2}\right] \quad (3.1)$$

r is the radial distance from the beam center, ω_0 the spot size (which is equal to the radial distance from the beam center where the intensity falls to e^{-2}). I_0 is given by

$$I_0 = \frac{2P}{\pi\omega_0^2} \quad (3.2)$$

Here, P is the power of the laser beam, which can be measured with the help of a power meter.

The two diodes are mounted in diode mounts (Thorlabs Inc.) in two different polarization directions, which is essential because the two laser beams are combined into one collimated beam by a polarization cube.

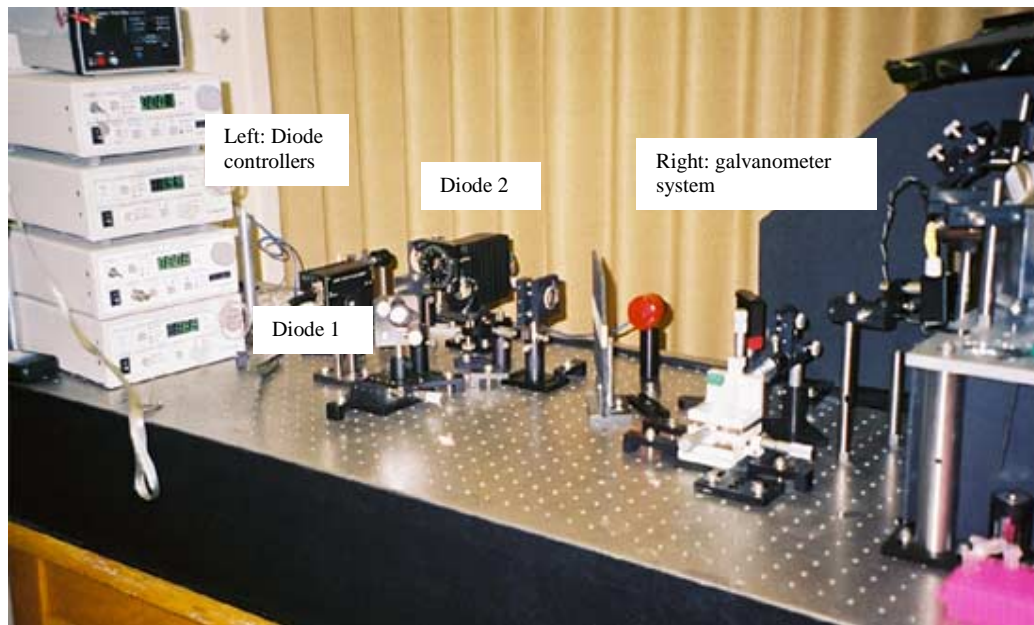


Fig 3.2: Setup of the optics

The wavelength of 810nm is chosen with respect to the absorption coefficient of water. Biological objects such as cells consist of ~ 80% water and show approximately the same absorption behavior than water. We want the cells to absorb the least amount of power as possible to minimize heating effects and therefore damage to the cells, so we chose the wavelength with a minimal absorption coefficient for water. Fig 3.3 depicts the absorption coefficient of water dependent on the absorbed wavelength of light:

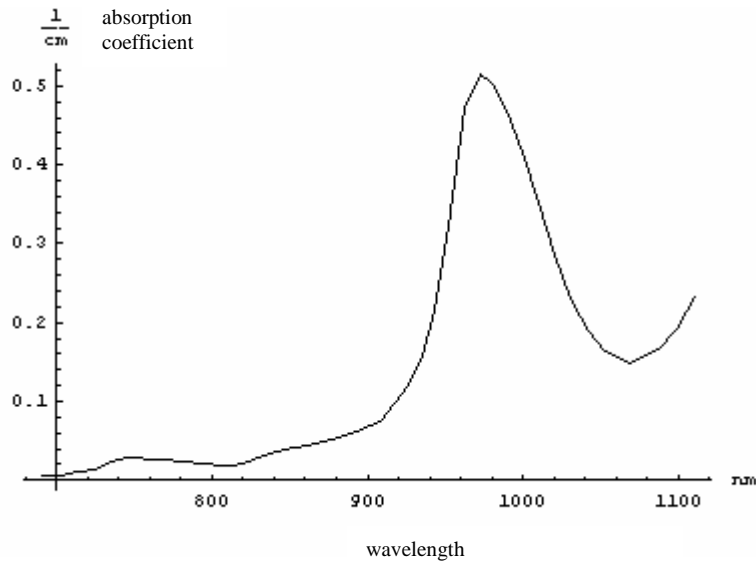


Fig 3.3: Correlation between the absorption coefficient of water and different wavelengths in the near infrared; datapoints from [38].

The two diodes taken together provide a maximum output power of $\sim 280\text{mW}$ before entering the galvanometer system (more in § 3.2.3). Due to the galvanometer mirrors, approximately one third of the total power is lost there. The objective, through which the laser light passes finally before reaching the cells, also absorbs power. So the final highest power available in our system is

around 100mW (these values are all empirical; measurements were all made with a Newport power meter)

With respect to the GT1 cells, it was also necessary to find out the threshold for any effects (specified in § 4, Results). Therefore we had to systematically run experiments throughout the whole power range. To achieve this, two attenuators (Melles Griot; optical density 0.5/0.8 at 546nm, or 0.4/0.77 at 810nm) were put in the beam path; this assures that the diode current does not need to be varied to a large extent, running the risk of reaching the threshold at which the diodes reliably emit coherent laser light (the diodes are specified to have a lasing threshold at a current of 25mA). The optical density D is defined as the base 10 logarithm of the reciprocal transmittance T [39]:

$$D = \log (1/T) \quad (3.3)$$

The final spot size in the focal plane, observed with the CCD camera, is about 1.2 μ m in diameter (corresponding to ω_0 in Eq. 3.1 and 3.2)

Fig 3.5 and 3.6 show the power measured after the objective (i.e. the focal plane) with two attenuators at different diode currents:

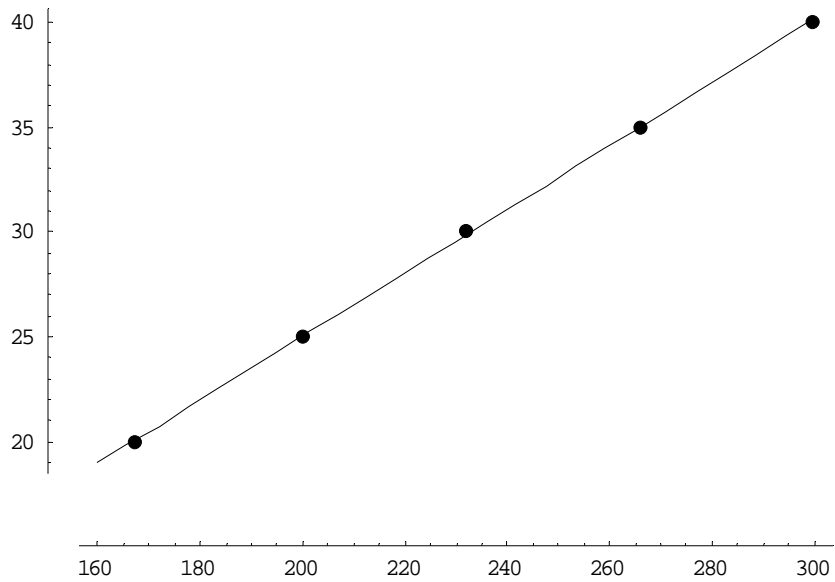


Fig 3.4: Power measurements with 0.5 (= 0.4 at 810nm) attenuator.
x-axis: current in mA (sum of both diodes)
y-axis: power in mW measured in the focal plane

Linear fit superposed with data points.

The linearity between current on the diodes and their output power is a typical feature of laser diodes

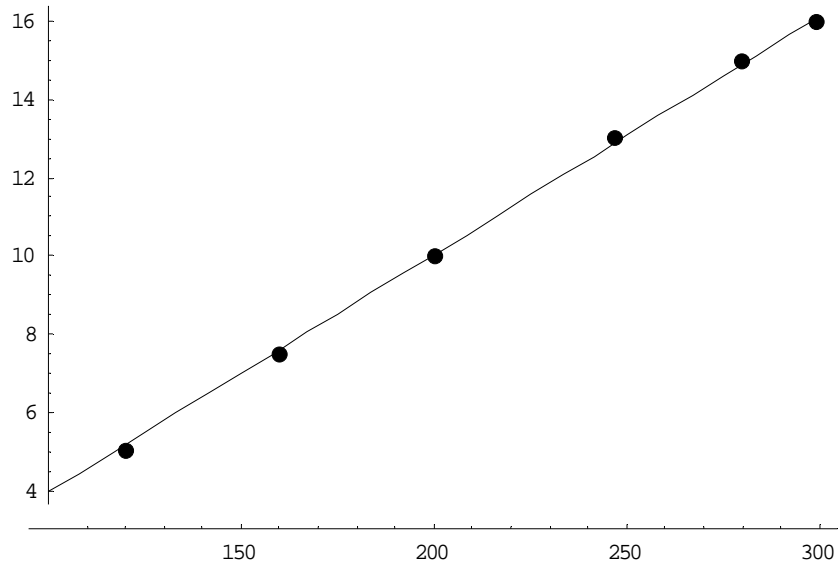


Fig 3.4: Power measurements with 0.8 (= 0.77 at 810nm) attenuator.
x-axis: current in mA (sum of both diodes)
y-axis: power in mW measured in the focal plane

Linear fit superposed with data points.

3.2.2 Optical elements on the beampath

As mentioned above, the laser beam has to pass through several optical elements for alignment and collimation purposes. The following schematic graph gives an overview of these elements:

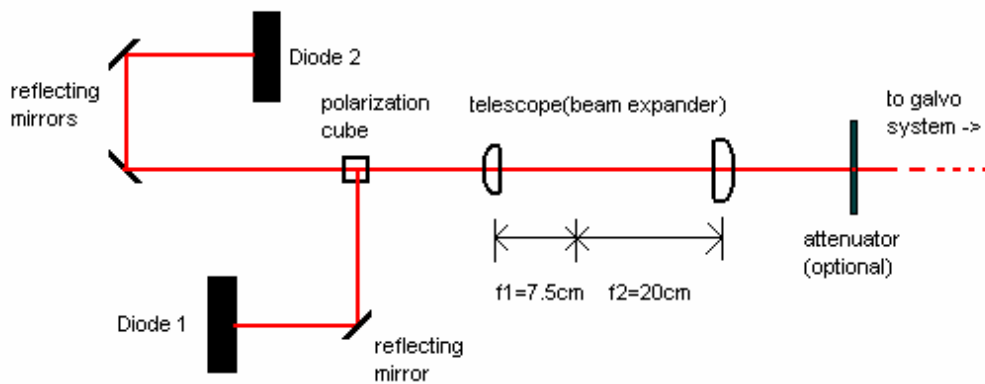


Fig 3.6: Laser beam path, schematic, as seen from top (drawing not to scale) with all important optical elements

As part of the setup at the beginning, or whenever an optical element has been changed, an alignment and a calibration is necessary. The first important step is to align the two laser beams right after they pass the polarization cube. For the alignment, the beams need to be iteratively superposed, which is done by

adjusting the reflective mirrors, right after the cube and in far-field ($\sim 2\text{m}$) until one collimated beam results.

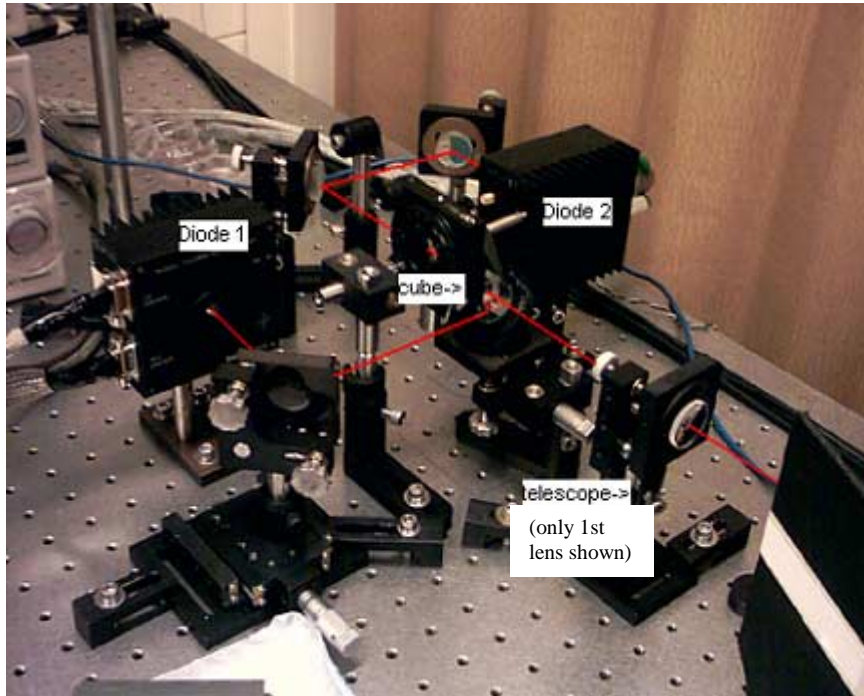


Fig 3.7: Laser beam path in reality

After this, a calibration needs to be done to ensure the galvos control the laser spot correctly. Therefore, the galvos are brought into their zero-voltage position (which corresponds to the laser beam being right in the center of all mirrors), and the laser beam also has to be centered in the aperture of the microscope's objective lens. The objective is then replaced by a cap with translucent paper bearing some ring marks in the center. Now, with the help of a Labview

program which controls the galvo positions, each position needs to be adjusted simply by viewing the laser beam and making sure it stays centered for all different positions.

3.2.3 The galvanometer system

To control the position of the laser focus in the focal plane with high accuracy, the beam passes a system consisting of four galvanometers (GSI Lumonics, M2 and M3 series) before entering the microscope. Fig 3.8 shows the position of the laser spot with respect to different mirror positions:

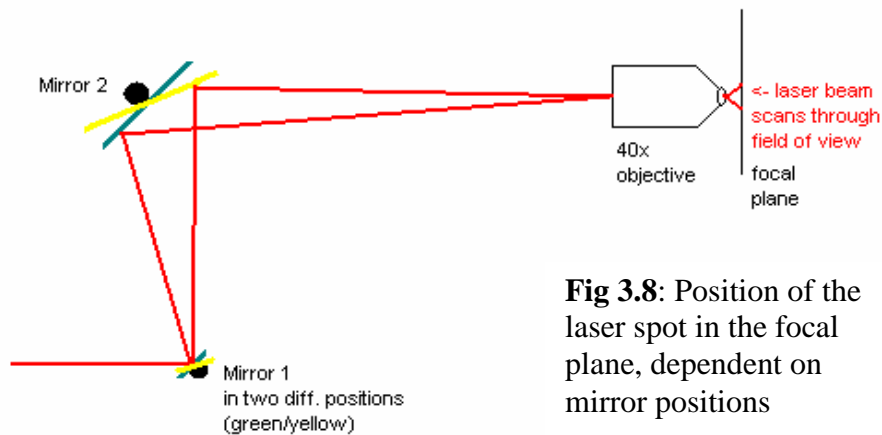


Fig 3.8: Position of the laser spot in the focal plane, dependent on mirror positions

Since there are two different directions (x and y) in the focal plane, which corresponds to two degrees of freedom, and every direction is controlled by two mirrors, we operate four galvanometers in total. Two of them are equipped with high reflectance gold mirrors, the other two with high reflectance silver mirrors.

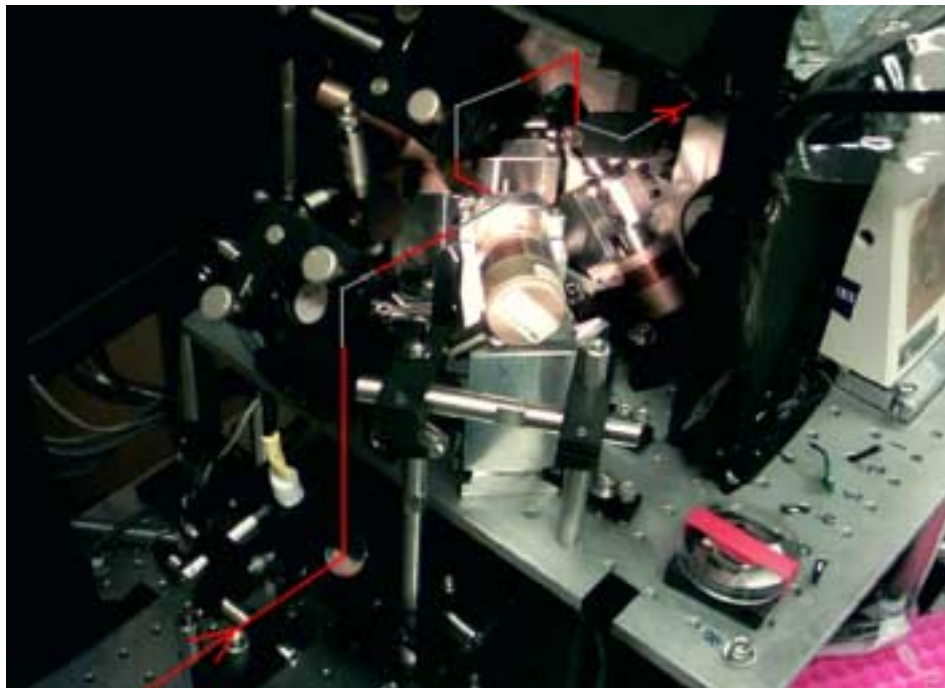


Fig 3.9: Beam path in the galvo system in reality (grey parts are hidden when path is viewed from this angle)

By using galvanometers, we have the possibility to set several laser foci at one time, since the mirrors can be moved with a dwell time of only 10ms between the different laser spots. Depending on the desired power for every spot, up to four spots can be set at the same time (total maximum power divided by the number of spots must not be smaller than the threshold power for any effects).

3.2.4 Microscope setup

Under a standard light microscope cells, or thin sections of tissue are examined by transillumination. Light is passed through a condenser that collects the light into a focused beam that then passes through the cells. Afterwards it is collected by a lens that magnifies the image (40x in our case). The cells are viewed through an ocular lens that also magnifies the image (10x). So the total magnification when viewing the cells through the microscope is 400x.

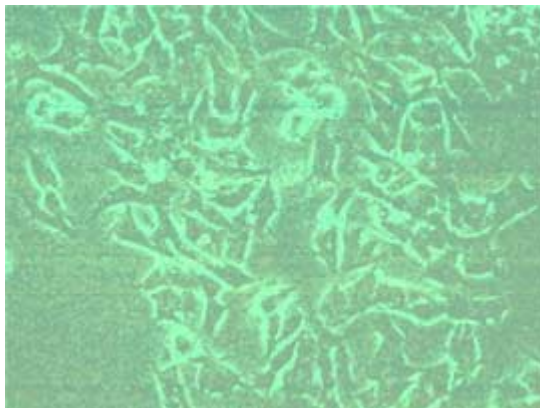


Fig 3.10: GT1-7 cells viewed through a standard light microscope; not many details are visible. Magnification ~ 100x

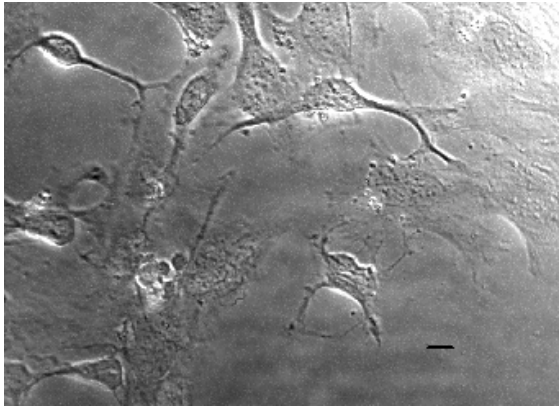


Fig 3.11:
GT1-7 cells in phase
contrast image; scale bar:
10 μ m

However, most cells and tissues in their natural state contain little pigment that would absorb light. Therefore, they are normally translucent to transmitted light and little detail can be seen. Consequently, other methods have been developed to make the details more visible. One of them is phase contrast microscopy, which we use in our system. Phase contrast microscopy can be used to image transparent cells. The principle behind this type of microscopy is that light changes speed and direction when passing through cellular and extracellular structures of different refractive indices. This causes some structures to appear lighter or darker relative to each other. The microscope used in our experiments is a Zeiss Axiovert 25, which is modified so that it is possible to either look at the cells through the ocular, or switch to the CCD camera for imaging.

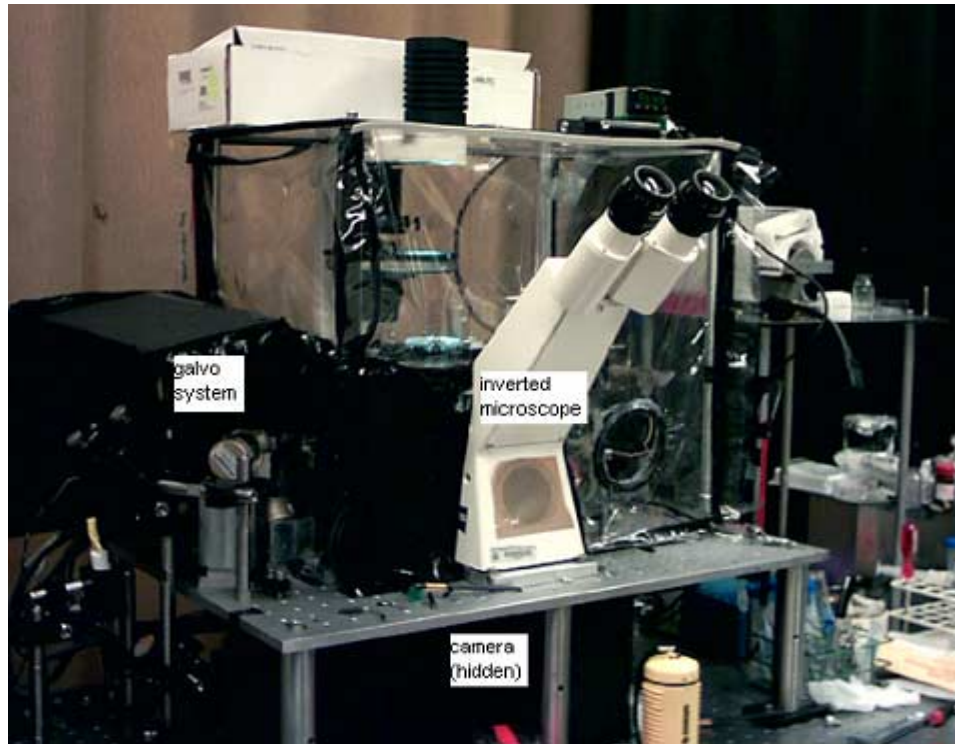


Fig 3.12: Microscope setup

The laser beam is expanded to fill the aperture of the back focal plane of the objective completely, and is then focused to form a $1.2\mu\text{m}$ spot size on the cells. The spot could be distorted by the phase ring in the objective. The phase ring is constructed so as to add a phase difference of $\lambda/4$ to make biological preparations visible. Only direct light beams are influenced by the phase ring, and thus some objects appear to have a light “halo” around them. The

maximum incident power at entry of the laser beam into the microscope is 180mW. After the objective (40x, Zeiss Fluor oil-immersion, NA 1.3, Ph3) we reach a maximum of ~100mW.

3.2.5 CCD camera

A CCD camera is attached right under the microscope to take pictures of the experimental run. The camera (AP9E , Apogee Instruments Inc., scientific grade) has an array of 3072 x 2048 pixels with a 9 μ m pixel size. For the actual image on the computer screen we can cover a field of view of 690 μ m x 460 μ m with a resolution of 0.6 μ m for the 40x objective.

3.3 Sample stage

For our experiment, a special sample stage was built by Samantha Moore to hold the experimental dishes and guarantee precise control. The dish can be attached firmly to it, and the position of dish and stage together are controlled by micrometer screws, which is especially important if, during an experimental

run, the dish needs to be moved within a few micrometers to adjust the picture on the camera. Furthermore, perfusion inlet or outlet tubes or coverslips can be easily exchanged during the experiment without moving the dish.

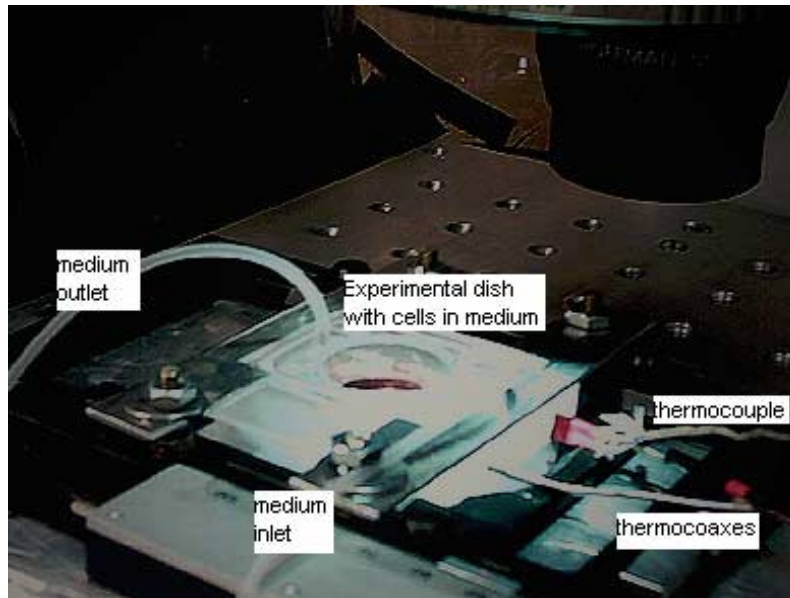


Fig 3.13: Experimental dish on the sample stage

3.4 Design of the experimental dishes

The perfusion dishes are also a special design for this experiment to ensure high cell viability and a good phase contrast image at the same time. Here the culture petri dishes would not be sufficient because the plastic bottom is too thick, and there is no possibility for heating as with the experimental dishes. The outer

material is lexan and a glass coverslip is glued with on the bottom (see below). On the two sides are inlet and outlet for perfusion of medium. For heating purposes, two thermocoax cables are inserted in the appropriate channels through the perfusion dish. The dishes are fully autoclavable.

Fig 3.14 to 3.16 illustrate the design:

drawing not to scale!

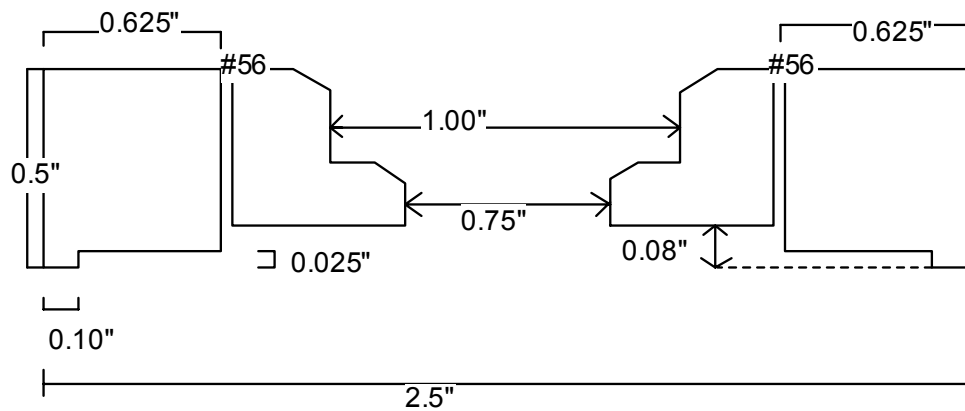
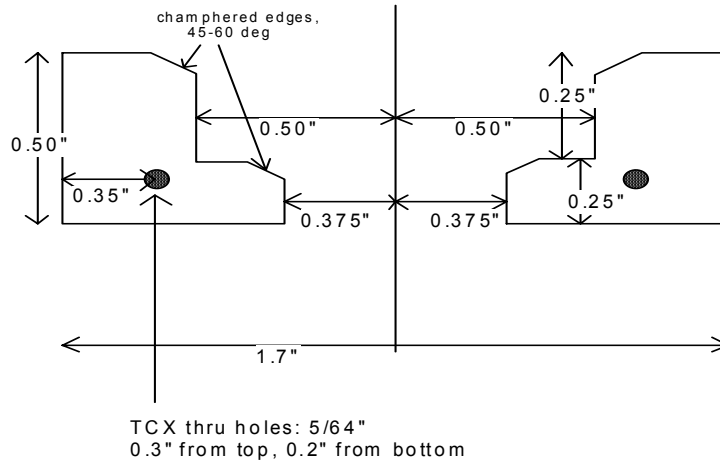


Fig 3.14: Side view of the experimental dish (long side)

drawing not to scale!



Top

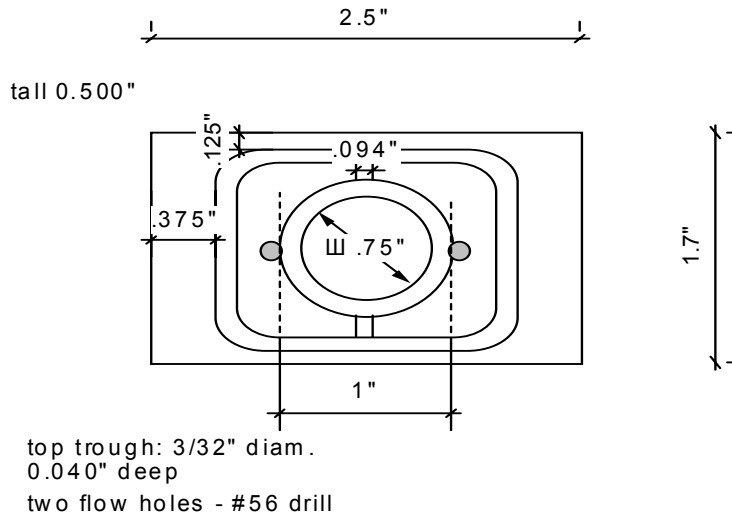
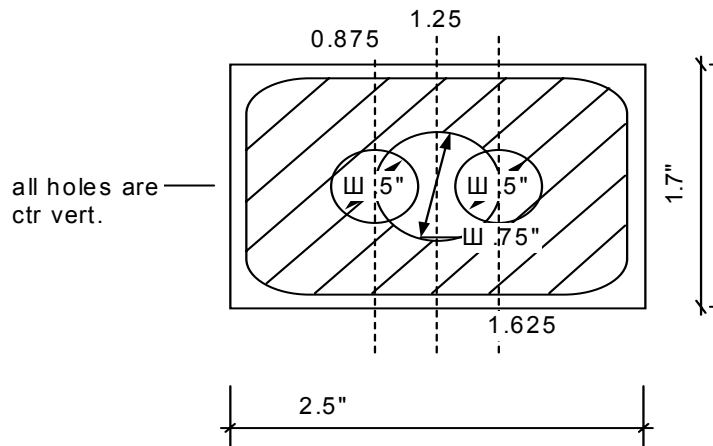


Fig 3.15: Side view (short side, upper figure) and top view (lower figure) of the experimental dish



flow antechambers: depth: 0.08" from lower surface
 coverslide trough: depth: 0.020" from lower surface
 0.1" from top/bottom/sides (see side view)

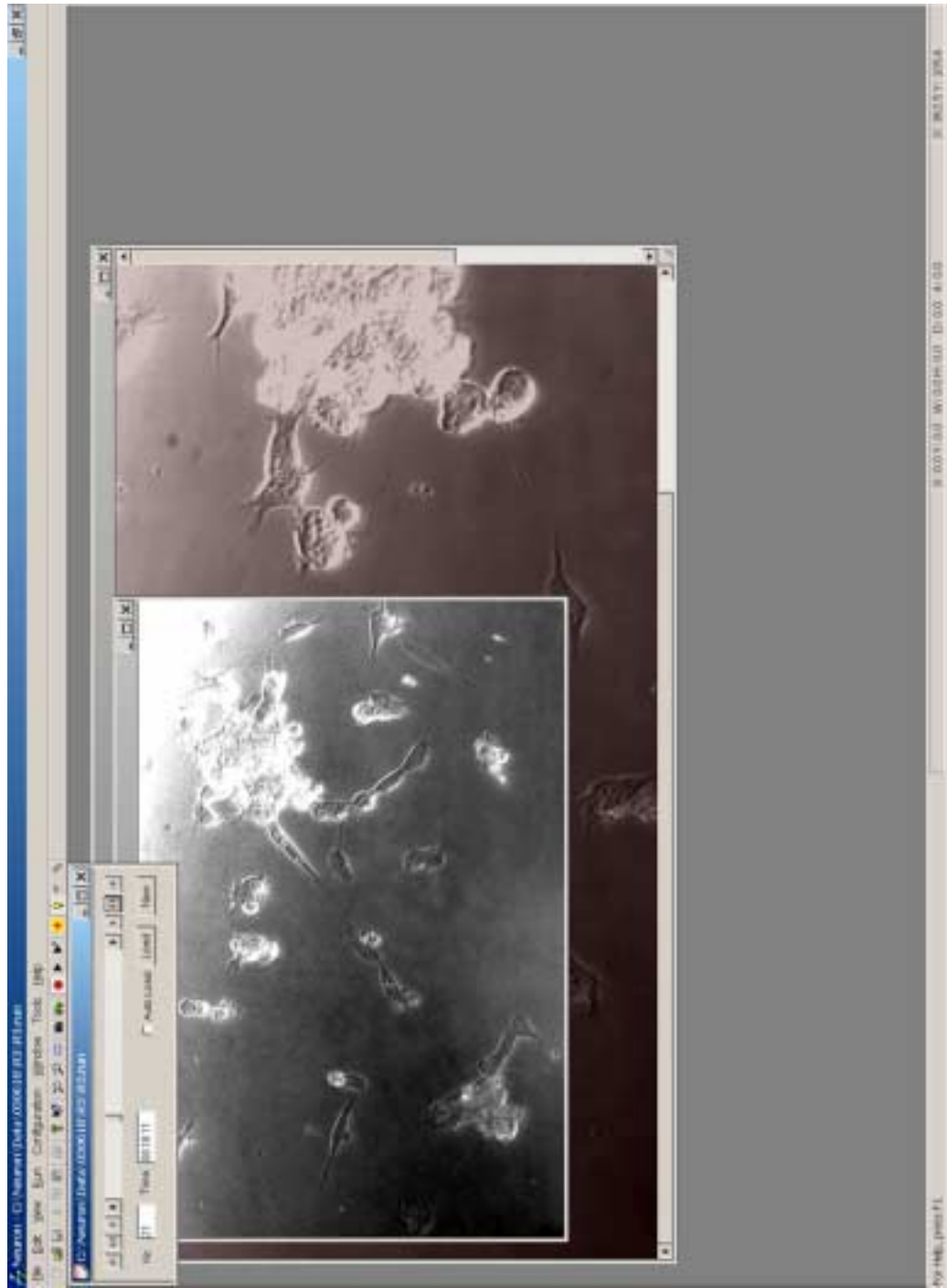
Fig 3.16: Bottom view of the experimental dish

For the experiment, a glass coverslip (24mm x 50mm) is glued on the bottom of the dish with RTV108 silicone glue. This glue has the advantage of not being toxic to the cells even after autoclaving, and it can be removed again very easily to replace the glass coverslip. For the medium inlet and outlet, syringe needles (size 18) are cut on both sides to form a small pipe and then inserted into the holes in the dish. Prior to plating the cells on the dish, it must be cleaned thoroughly with bleach, millipore water and finally 100% ethanol and

autoclaved for at least 30 minutes at 125°C. Cells are then transferred from their petri dish or flask (see also cell culture procedures – plating) and grown for several days on the glass coverslip until they reach about 50-60% confluency. The last 2-3 days before the experiment the culture medium should be replaced by serum-depleted medium. Culturing cells in medium depleted of serum leads to inhibition of cell division and increased extension of neurites [21].

3.5 The Neuron program

This computer program, written in C++, was developed by Florian Schreck especially for this experiment. Its main purpose is to gain complete control over the CCD camera functions like the picture taking cycle, shutter delay, and desired field of view. Furthermore, when guiding cells like the NG108, it provides an option for recognizing the outline of cells and place the laser spot on the tip of the growth cone accordingly. This so-called ‘detection picture’ is taken every time in addition to a ‘cell picture’ and a ‘laser picture’. The most important features shall be presented on the next two pages with the help of screen shots:



Previous page:

Fig 3.17: Basic screen during a run

The picture in the background represents the currently loaded picture, including laser picture and detection image (not visible). The smaller picture is only loaded as cell picture, thus it is easy and fast to scan through all the pictures taken during a run and then load a specific one (or several) if desired with the help of the little dialog box on top. This dialog box either shows the current picture during a run, or, if the data file is reopened later, provides the number and actual time during the run (more on the dialog box on the next page). All pictures are saved on harddisk during a run, and can be accessed again at any time with the Neuron program. It is also possible to print out pictures with the 'print' option in 'file' or to choose a small frame of interest and save this area throughout all pictures as BMP (bitmap) file; this is important when compiling all pictures from the run into an avi movie (see Appendix B).

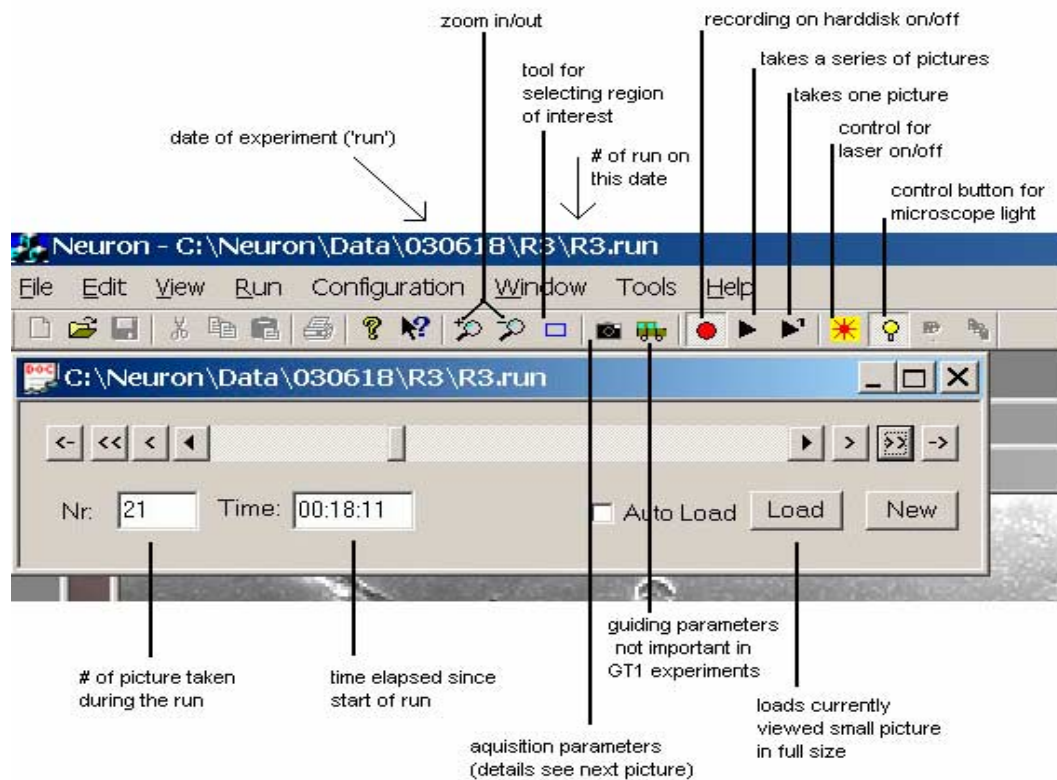


Fig 3.18: Details on the dialog box and the control buttons

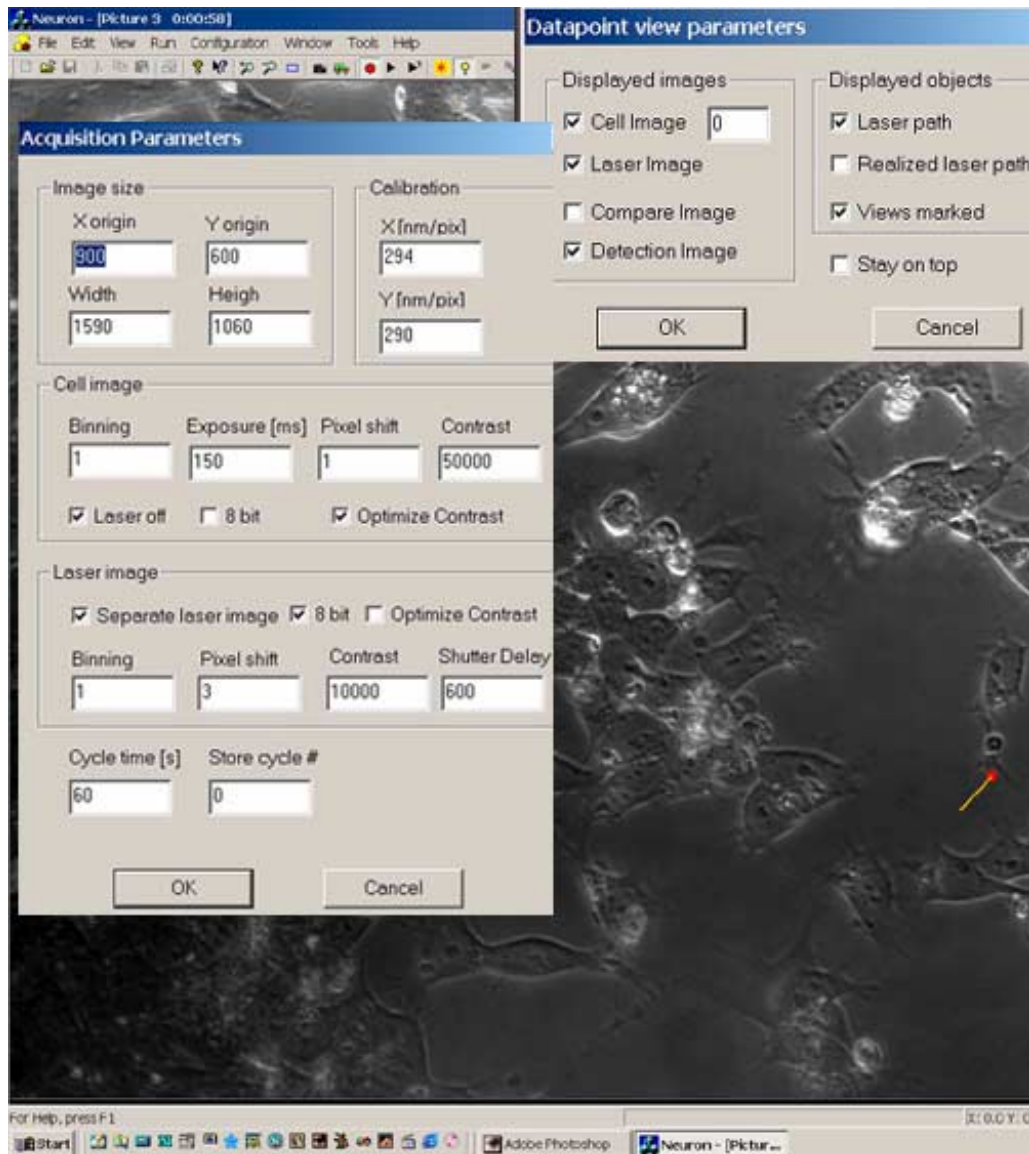


Fig 3.19: Computer screen during an experiment (background). The red square (plus yellow line) indicates the position of the laser spot Superposed: two dialog boxes; details see next page

The left dialog box is the acquisition parameter control, which allows the user to choose any field of view during the experiment (in pixels). The calibration values are firm and are important for determining the magnification of the picture and also growth distances of the cell's axons. The controls in cell image and laser image allow variations in pixel shift, exposure time (actual time the shutter of the camera is open to take a picture), contrast, and shutter delay. The cycle time gives the delay between one picture and the next.

Furthermore, with a right-click on the mouse, a dialog box for datapoint view parameters appears, where different 'layers' of a picture can be made visible. The cell image is always superposed on the laser picture, and the laser picture superposed on the detection image. For the GT1 experiments, a detection picture was always taken, but not used any further. By turning the pictures off one after another, the desired picture can be viewed. The option laser path corresponds to the red square, which also can be taken away if desired.

3.6 Preparations and setup of an experimental run

Before a run (and thus the work with the Neuron program) can be started, several setup procedures are necessary. In order to keep the cells at 37°C until the thermocoaxes are finally connected to the experimental dish, we warm up a cooling aggregate to 37°C in the water bath, and also 2.5 – 3ml run medium (consists of CO₂-independent medium from Gibco, + 10ml pyruvate and 10ml L-glutamine and 5ml N2-supplement (Gibco) per 500ml). With the help of the warm aggregate, cells are then transferred from the incubator in the cell culture room to the sample stage on the microscope. Before putting the dish on the microscope, one drop of oil needs to be placed on the objective lens. The serum-depleted medium in the experimental dish is replaced with the run-medium, and a round 25mm glass coverslip, cleaned with 100% ethanol, is put on top to prevent evaporation of medium and possible contamination by bacteria. Careful attention has to be used so that no air bubbles remain below the coverslip, because images taken with the camera will then be distorted by reflections caused by the air bubbles. After that, the two thermocoaxes are inserted into the dish and connected, and a thermocouple is placed very near to one of the thermocoaxes for monitoring the temperature. If using perfusion,

some additional run medium needs to be added to a flask; silicone tubing (autoclaved) as medium inlet and outlet is then connected to the dish, and the ingoing medium is also heated to 37°C with a thermocoax (see Fig 3.13). First, the inlet tube is connected, and the peristaltic pump started in reverse mode so that medium is running back in the tube until no air remains. Then it is switched to forward again, providing fresh medium, and the outlet tube needs to be connected to keep the medium level constant.

Now some suitable cells can be sought first under the microscope, then the Neuron program can be started for the actual data acquisition.

However, if not perfusing constantly, it is possible with the help of a syringe and a 25G needle, to take out ~1ml medium through the inlet or outlet hole in the dish at any time during the experiment, and refill with new medium.

According to our experience, the cells do well even after several hours without new medium; however, it has been reported that simple exchange of medium at any time encourages filopodial activity [40]. On the other hand, constant perfusion can wash away neurotransmitters; so, with the GT1 cells, we worked without perfusion in most cases.

Chapter 4

Results

4.1 Introduction

Our initial aim with the GT1 cells was to show that the technique of optical neuronal guiding also works with these cells, to try to guide them, and maybe build up small neuronal networks. However, as shall be seen in the next two chapters, the GT1 cells show a different response to the laser than the NG108 and PC12 cells before.

GT1 cells clearly do not grow into the laser focus. Instead, in most cases, we could observe a morphological change of the growth cone, sometimes resulting in cell body movements while the growth cone itself remained in the same place as before.

The occurrence of this new effect clearly does not meet our expectations, but could reveal valuable insights into the mechanisms underlying optically guided neuronal growth (see also §5).

This chapter is intended to present the results of our experiments and show the most striking examples.

Also, because these kinds of effects have not been seen before with the other cell lines, we tried to get statistically relevant data on how often the cell responds to the laser with what morphological change, and the power range for which this occurs. Thus, for comparisons among the experiments it was important to maintain the same experimental conditions. After some initial variations in culturing, it turned out that cells which have been growing on the experimental dish for 3-5 days (which corresponds to 2-4 days in serum-reduced medium) show the highest viability and a high rate of neurite extension at the same time. Also, GT1 cells need a thin layer of extracellular matrix protein to attach to, in our case laminin (1 μ g in 1ml medium in the experimental dish during culture). Attempts to culture GT1 without any addition of laminin failed. However, higher concentrations cause the cells to be more motile and thus less suitable for experiments.

The passage number (we used cells between 8 and 16) also did not seem to have any influence on the outcome of the experiments.

4.2 Induced morphological changes

A cell's growth cone can take on different shapes during axonal elongation, depending on its activity. In a more active phase, the growth cone is flattened and has ruffling lamellipodia and active filopodia scanning the environment for chemical cues or nearby cells in order to find the 'right way'. When less active, the growth cone exhibits a more rounded shape, or it even retracts in case of a negative feedback from the filopodia. *In vivo*, this behavior ensures that the axonal tip reaches its exact final destination, interpreting all external environmental cues, and establishes synapses with the correct cell. Neurite outgrowth always occurs in alternating phases of resting and protrusion. In case of the GT1 cells, these morphological changes occur also naturally, since these cells exhibit spontaneous action potentials in a certain time scale which is associated with a pulsatile hormone release [42]. Thus there is a possibility to interfere with these spontaneous action potentials.

In order to define a morphological change in a growth cone, we first need to look at different growth cone shapes and what they tell about the level of activity in the growth cone.

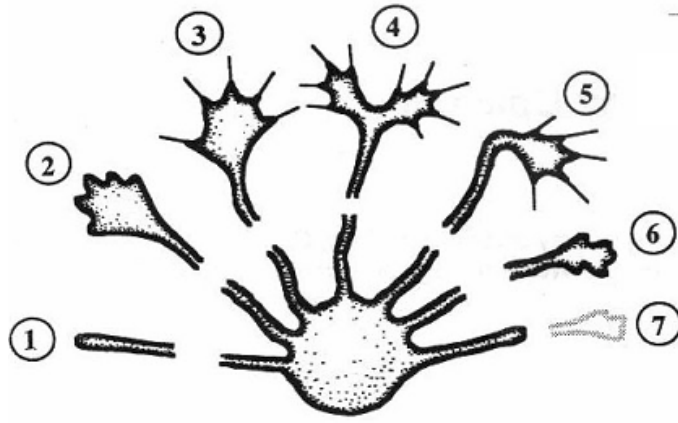


Fig 4.1: Schematic representation of neuronal growth cone behavior during events such as pathfinding and circuit formation. These behaviors depend upon the intrinsic state of the neuron and the environment that the growth cone encounters. 1, outgrowth in the absence of filopodia and lamellipodia is observed both in cell culture and *in vivo*. 2, outgrowth with a distinct lamellipodium but without filopodia. 3, the most commonly encountered form: a broad flattened lamellipodium with many filopodia. 4, branching is observed, both spontaneous and in response to evoked stimuli. 5, turning, evoked or spontaneous, is observed in cell culture and *in vivo*. 6, arrested forms of growth cones can be observed with or without filopodia extended. These arrests may be permanent or may represent transient pauses in the motility of the growth cone. 7, retraction as a response to a ‘stop signal’. Adapted from [41]

As mentioned above, our experiments were initially intended to induce enhanced neurite outgrowth, as in the NG108 and PC12 cells. Thus we also chose visibly active growth cones with ruffling lamellipodia. To maintain equal conditions as well as possible, the growth cones chosen initially looked alike.

However, one could make a difference in either choosing a cell within a cluster, located somewhere at the boundary, or a single cell which is not influenced directly by others.

It turned out very soon that GT1 cells do not respond to the laser in the way we expected. None of them showed a tendency for enhanced growth; in contrast, we observed in most cases that the initially active growth cone did undergo a quite rapid change in morphology. Growth cones with lamellipodia and filopodia usually rounded up within up to 15 min; afterwards, the cell body showed a tendency to pull itself backwards (opposite direction of the growth cone), causing the axon to elongate and in some cases also to become thinner, whereas the growth cone itself remained in the same place, where the laser spot was also located. Interestingly, this effect did not occur when the laser was placed on a dendritic protrusion: here the cell responded with mere retraction away from the laser. Also, moving the laser spot along the cell membrane on the growth cone did not alter the effect, while moving the laser orthogonally to the membrane (inwards or outwards) weakened the effect if not inhibited it completely. Adding laminin to the run medium, or replacement of the run medium after several hours did not cause any changes in these observations. Two experiments with constant perfusion did not alter the effect either.

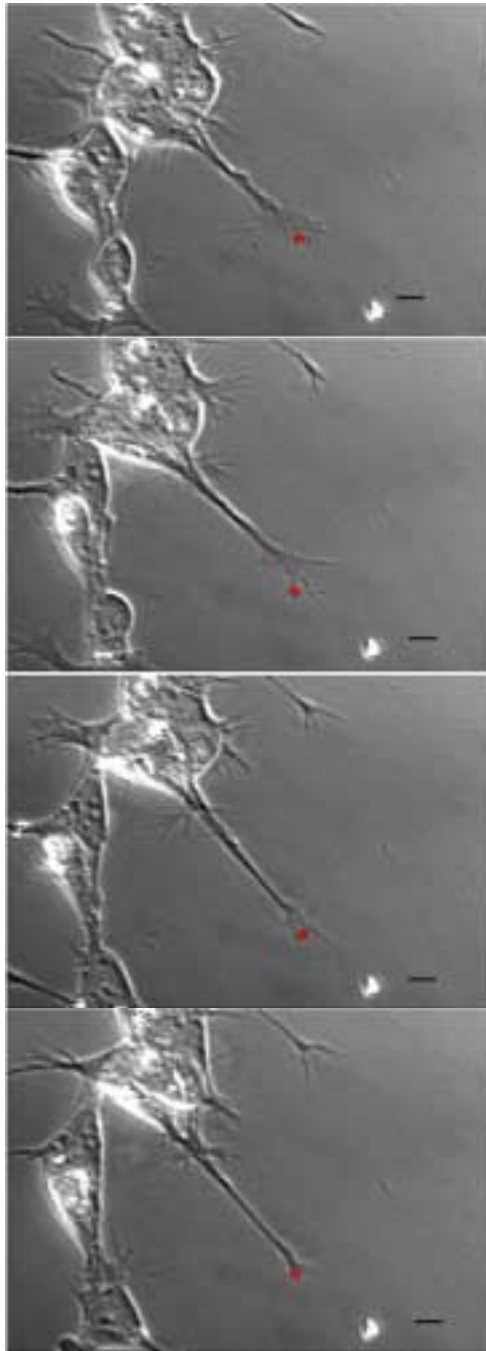


Fig 4.2: GT1-1.

Induced morphological change in the growth cone. Initially flattened with several filopodia and lamellipodia, the growth cone shows a rounded shape after about 15 minutes. Also, the cell body is moving backwards, causing the axon to become longer and thinner. Time period: 20 min. Time interval: 5 min. Scale bar, 10 μ m
Laser power: 20mW

This applies for these and all following pictures: the red laser spot was inserted afterwards for picture quality reasons. It reflects the original position, but not necessarily the exact size (although fairly accurate). Spot sizes in reality varied between 1.1 μ m and 1.5 μ m diameter.

In some cases, the cell also retracted its protrusion completely after some time, regardless of the laser beam. Then a new growth cone on another cell was chosen. A new cell was also chosen after about 20 minutes when the cell body was eventually moving back, with no new changes in the growth cone. Nothing happened when a growth cone with an already round profile was chosen, so we restricted the search to growth cones with extended filopodia and lamellipodia. The cells could be maintained without change in viability for up to 10 hours. Then a slight decrease in activity, i.e. less neurites extended, was observable. The laser spot was set on the membrane so that about $\frac{1}{2}$ was outside the cell, and $\frac{1}{2}$ inside. Like this, the intensity is highest directly on the plasma membrane because of the Gaussian profile of the beam. Laser powers were varied between 96mW and 5mW in order to find a threshold for the observed effect. It also could have been possible that the cells show other responses, maybe even growth like the NG108, at lower powers than 96mW. It turned out that there seems to be a threshold power of around 20-25mW for the cell to show a response at all, above which the effect of the growth cone rounding up could be observed, below, however, the cell did not seem to be influenced by the laser. The following table summarizes the different observations and how often they occurred:

GT1-1	Observation	Number of cases	Laser power
	Growth cone is rounding up, but remains in the same place; Cell body moving backwards	24	16-96mW
	Axon retracts completely	2	96mW
	Growth cone rounds up at first, reextends after laser has been turned off	4	50-96mW
	Dendrite retracts	9	5-96mW
	Varicosity builds up, moves backwards along the axon	7	10-50mW

	Axon retracts and reextends at another place on the cell membrane	2	50mW
	Growth cone undergoes several shape changes, but stays in the same place	2	16-50mW
	Growth cone rounds up and stays in the same place even when another cell pushes the axon away	6	40-96mW (single case at 5mW and 10mW)
	Growth cone stays in the same place, while cell establishes several synapses to other cells in other places on the membrane	1	20-70mW

	Cell shows no discernable response to the laser	6	5-20mW (single case at 40mW)
	Cell is influenced by nearby cell, thus is not counted	8	5-96mW
GT1-7	Growth cone stays in same place, cell body moving in random direction	4	96mW

Table 4.1: Experimental results

If a cell showed more than one response of all listed in the table, it is counted according to the number of different responses. Taken together, the experiments show in 85% of all cases a “positive” outcome, meaning that the cell responded in a similar manner. The cases in which the axon retracts, or when no reliable response to the laser could be observed were counted as “negative”. The cases in which the laser was put on a dendrite and it retracted, or when the cell got

influenced by a nearby cell via synaptic contact of any kind, were excluded from these statistics. For the GT1-7, only four experiments have been conducted so far, and all showed results similar to the GT1-1, namely that a growth cone stays in the same place, while the cell body moves backwards. However, with the GT1-7, these observations are not as clear as with the GT1-1, since GT1-7 attach more firmly to the coverslip, even without laminin, and any movements or growth behaviors are hard to detect.

As the table shown above implies, these different observations were not strictly independent of each other; indeed, some of these descriptions are “aggravated” cases of another one. For example, the case in which another cell’s axon tries to cross the path of the axon the laser is influencing, and despite the other cell’s actions the growth cone shows the same morphology changes and eventually stays in its place, this is even more evidence for the effect described first in the table. Another example is the cell depicted in Fig 4.9, where the cell even seems to establish synaptic connections to the nearby cells, whereas the growth cone stays with the laser.

A clear difference in behavior between single cells and cells within a cluster could not be observed.

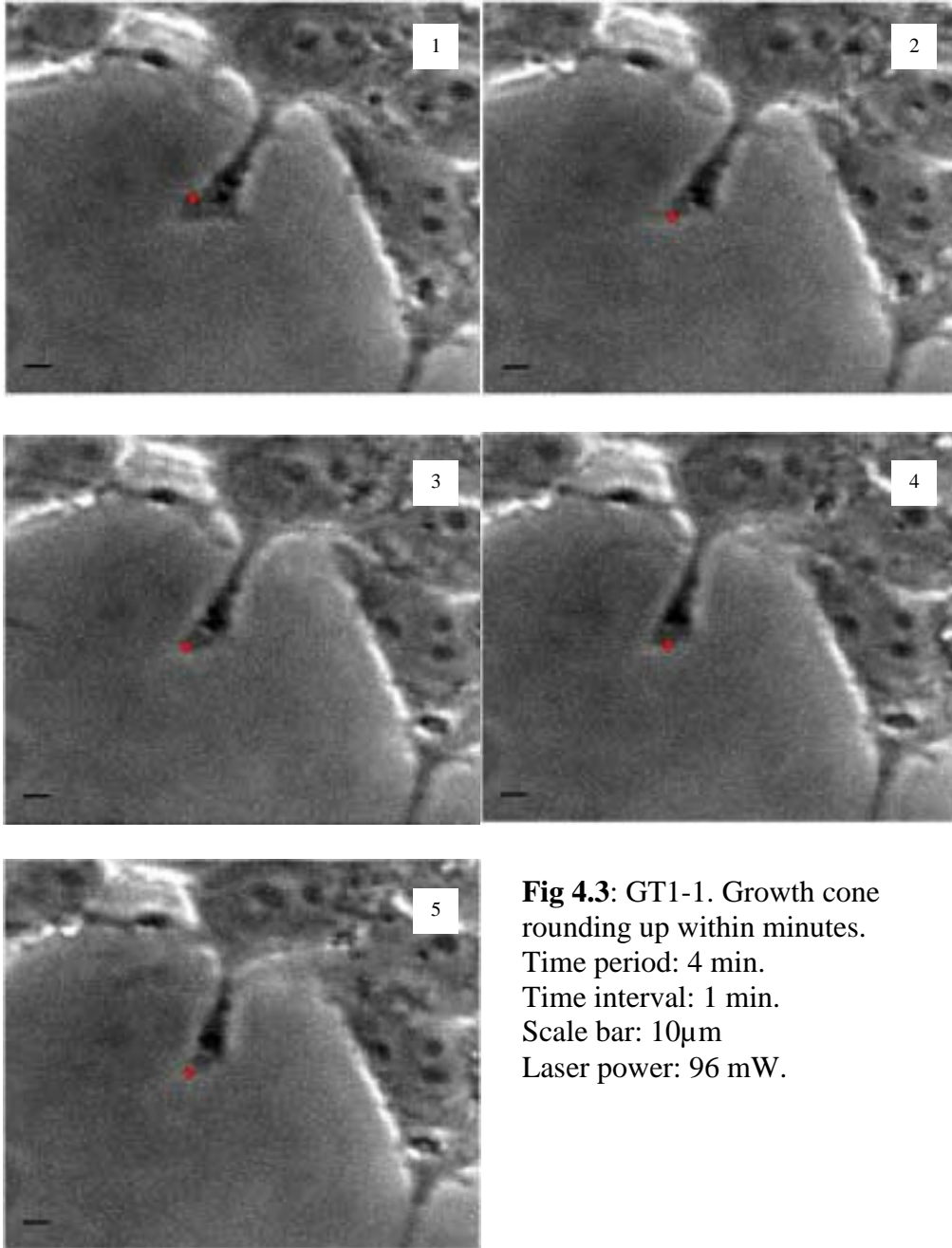
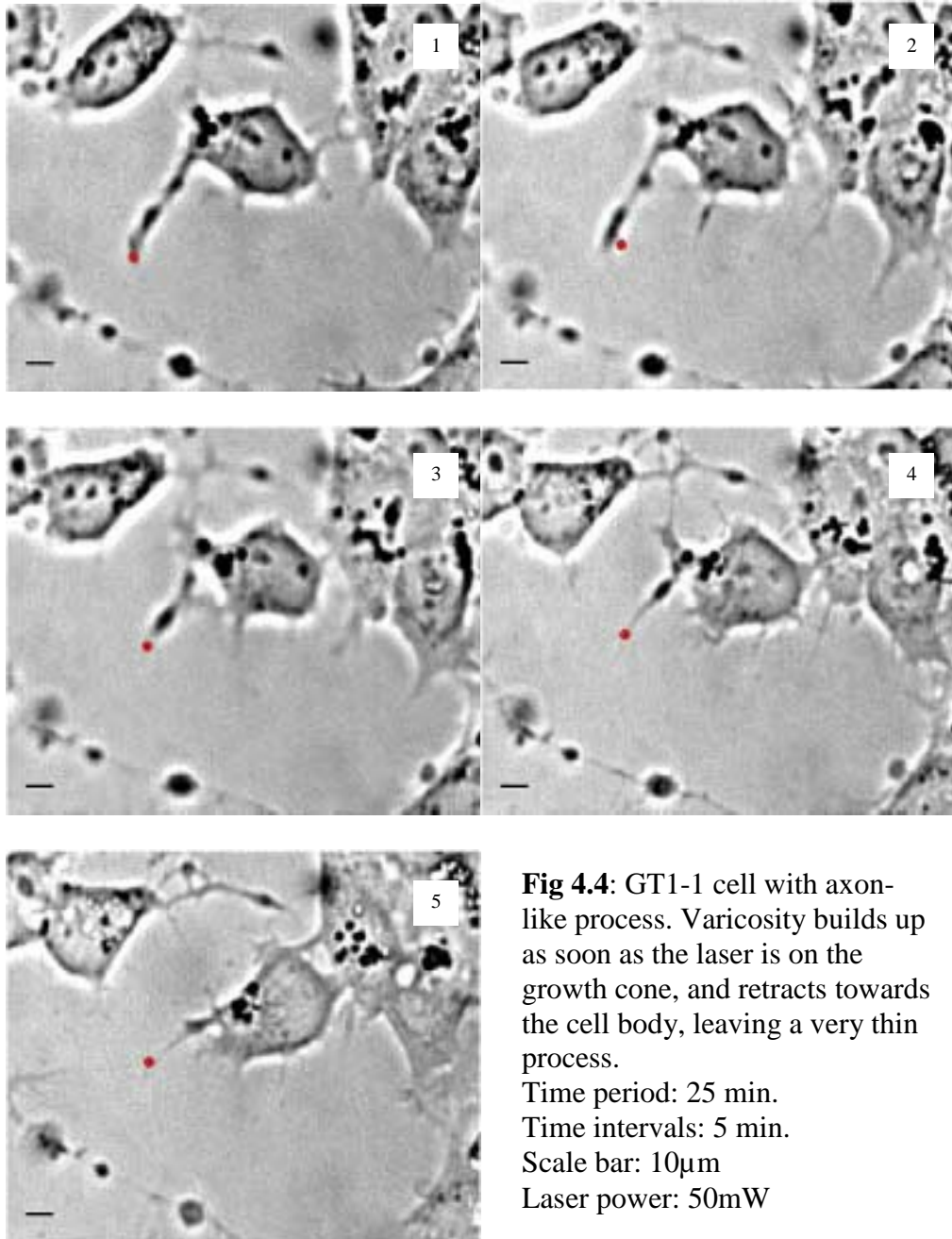


Fig 4.3: GT1-1. Growth cone rounding up within minutes.
Time period: 4 min.
Time interval: 1 min.
Scale bar: 10 μ m
Laser power: 96 mW.



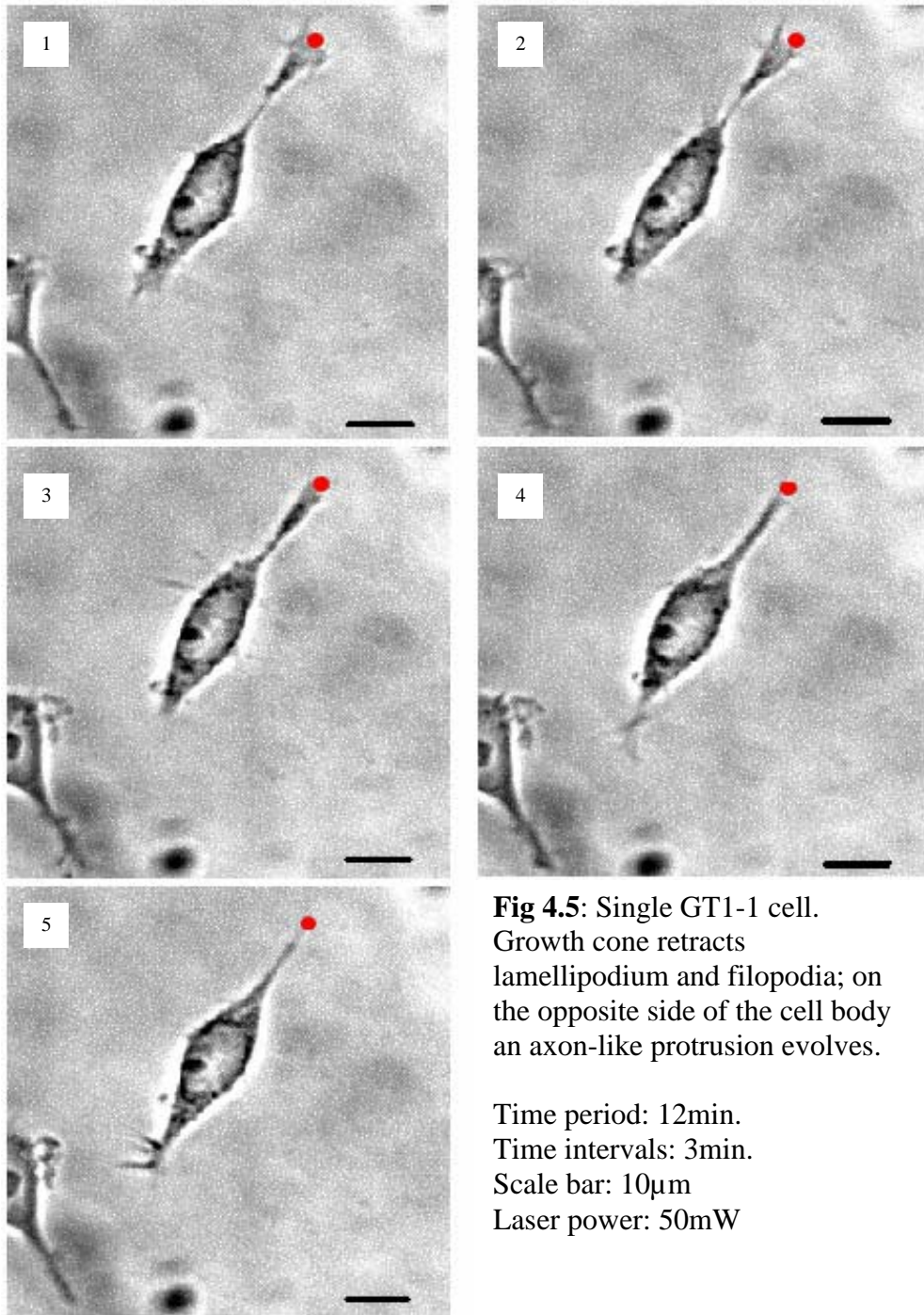
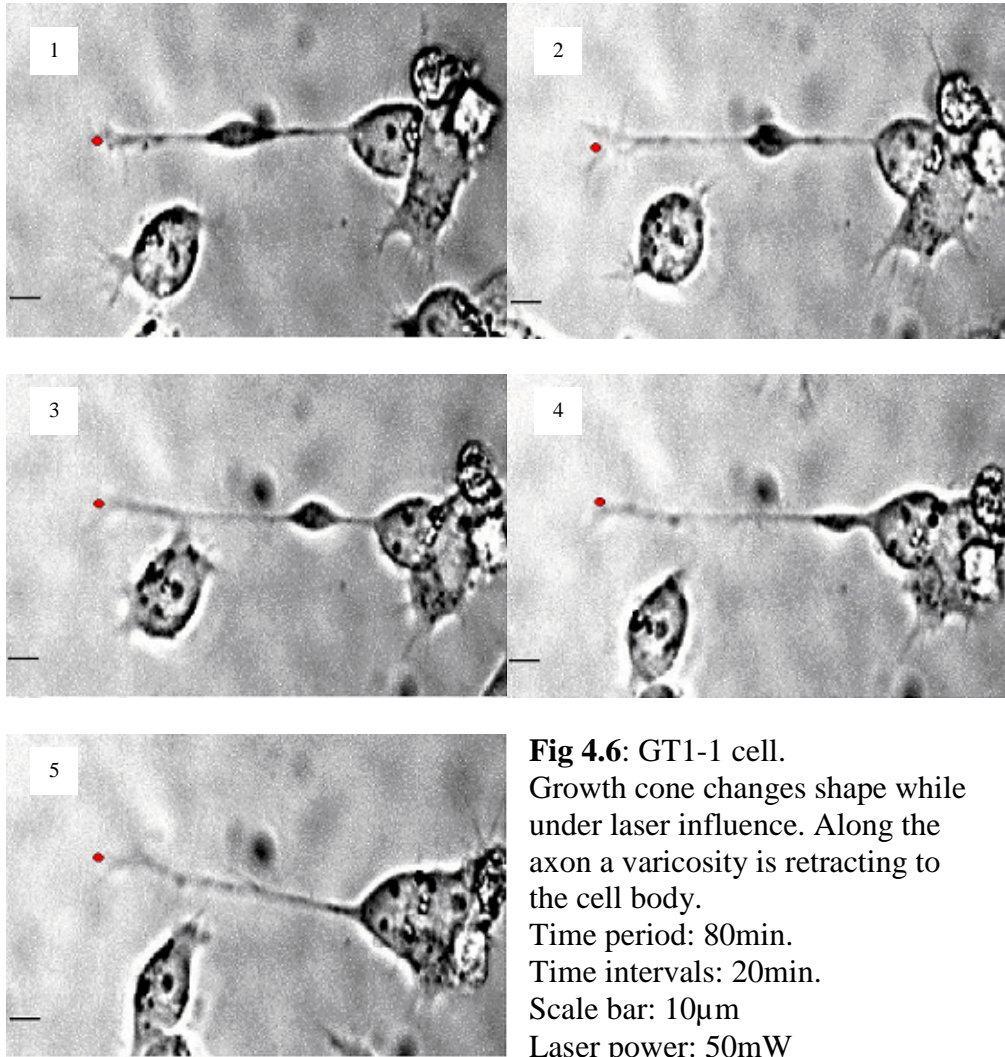


Fig 4.5: Single GT1-1 cell.
Growth cone retracts
lamellipodium and filopodia; on
the opposite side of the cell body
an axon-like protrusion evolves.

Time period: 12min.
Time intervals: 3min.
Scale bar: 10 μ m
Laser power: 50mW



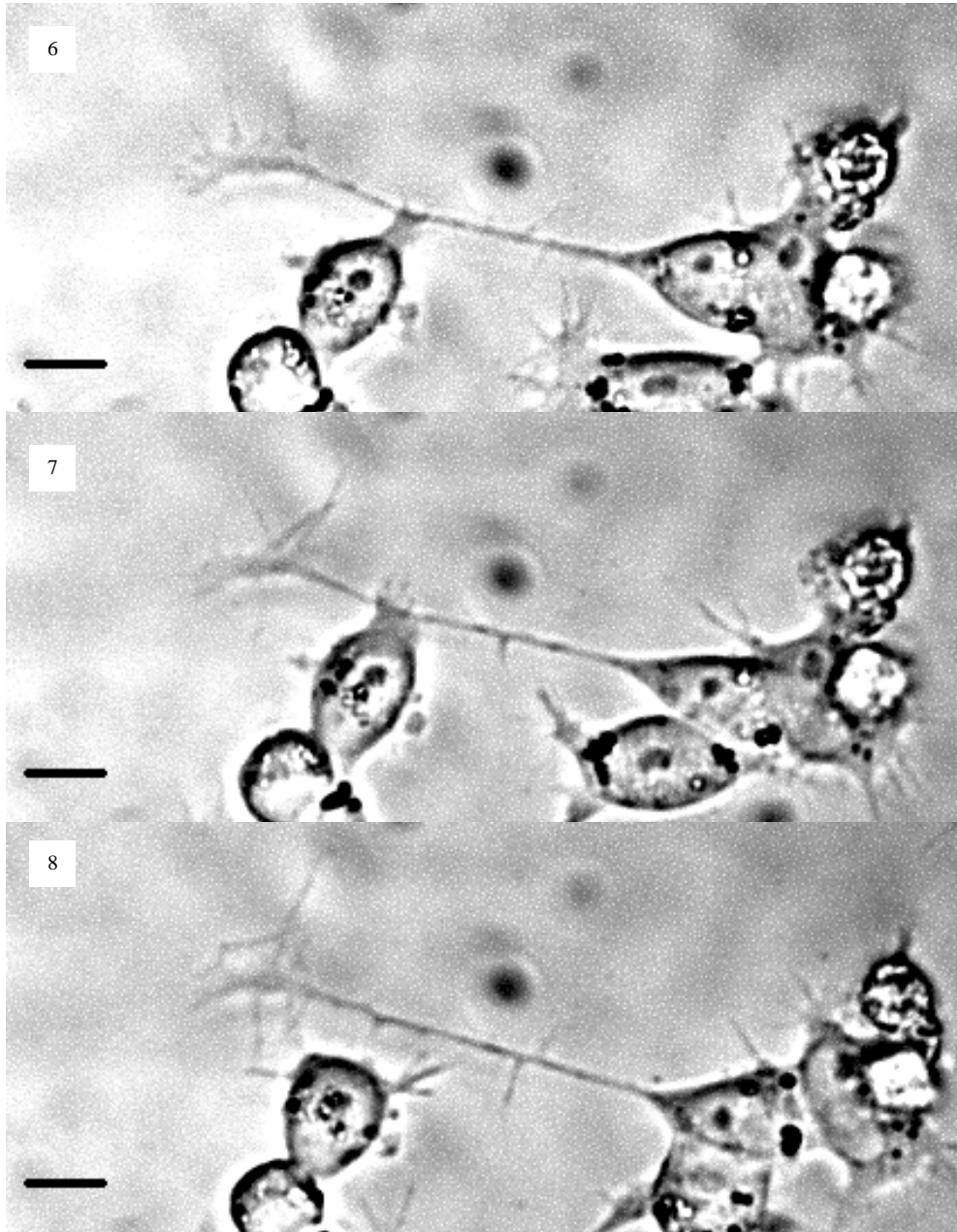


Fig 4.7: GT1-1 cell, reextending. The same cell after the laser has been turned off (pic 5-pic6: 56 min). Clearly visible are very active filopodia again. Time period: 30min; time interval: 15min, scale bar: 10 μ m.

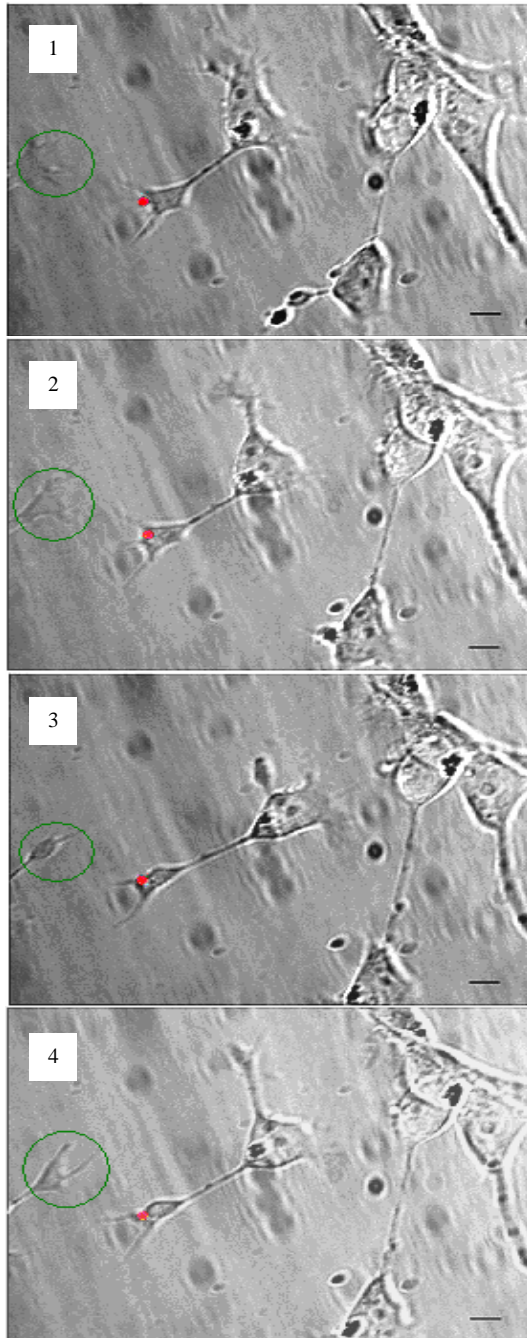


Fig 4.8a: GT1-1 cell, connections.

Single sitting at first and with large lamellipodium and several filopodia at the growth cone, this cell seems to make synaptic contact with two other cells while the growth cone undergoes shape changes, but does not move.

Notice also the cell in the green circle on the left, which is morphologically very alike, but not influenced by the laser; it starts to exhibit the same changes in the growth cone, but retracts completely within a short time.

Time period (1-3): 12 min.

Time interval (1-3): 4min.

(3-4): 5min.

Scale bar: 10 μ m

Laser power: 50mW

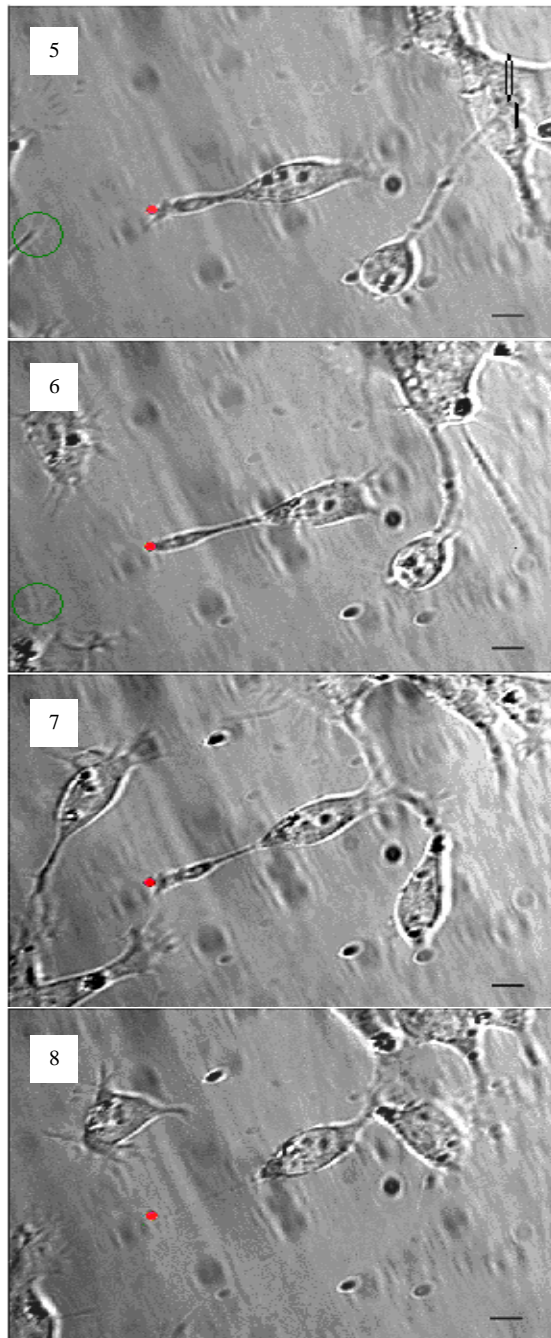


Fig 4.9b: Fig. 4.9a continued.
Here the cell body starts moving backwards and eventually seems to connect to the other cells.
Time period (4-8): 80min.
Time intervals (4-8): 20min.
Scale bar: 10 μ m
Laser power (5): 40mW
Laser power (6): 30mW
Laser power (7+8): 20mW

Chapter 5

Discussion and theoretical considerations

As described in the previous chapter, our experiments showed that GT1 cells exhibit an unexpected and “so far unexplained“ behavior in terms of optical guidance. This chapter is intended to discuss another approach to the underlying mechanism and possible aims for further experiments, since we are still at the beginning of optical guidance experiments on these cells.

5.1 Intrinsic mechanisms in GT1 cells

For more than a decade now, GT1 cells have provided a very useful model for studying immortalized hypothalamic cells *in vitro*, and many of their intrinsic mechanisms have already been revealed. The most important one is probably their spontaneous pulsatile inter- and intracellular calcium waves [42]. Here a difference between the GT1-1 and their sister clone GT1-7 becomes apparent, as the GT1-1 exhibit intercellular calcium waves, while GT1-7 have shown to generate intracellular calcium waves. The intercellular waves in the GT1-1 are

proposed to be generated by calcium-influx primarily caused by the propagation of depolarization via gap junctions and the waves propagate at a rate of 100 to 240 μm per second over groups of 100 to 200 cells. All spontaneous increases in calcium could be abolished by removal of calcium in the perfusion medium, or by addition of tetrodotoxin (TTX), a sodium channel blocker. Calcium waves in GT1-1 are thus dependent on the influx of extracellular calcium and somehow linked to sodium channel activity.

In a cell cluster of about 50-100 cells, the calcium waves were repeatedly initiated from the same 3-8 sites; these cells were termed 'pacemaker cells'.

Several other studies show that K^+ -channels in the plasma membrane induce a depolarization which leads to this cytosolic increase in calcium, and that also several types of Ca^{2+} -channels are present in at least the GT1-7 subclone [31]. These channels are suggested to be, at least in part, responsible for the release of GnRH, since coupling of $[\text{Ca}^{2+}]_{\text{cyt}}$ (intracellular/cytosolic calcium concentration) and the secretion of stored neurotransmitters or hormones, such as GnRH, is ubiquitous across secretory cell types like GT1. GnRH secretion from GT1-7 neurons is also pulsatile with ~ 1.28 pulses per hour and 20 minutes pulse duration. Little is known about the mechanisms underlying this pulsatility, but the periodic alternations in $[\text{Ca}^{2+}]_{\text{cyt}}$ could be responsible for this

phenomenon [43]; GnRH secretion and calcium oscillations are chronologically tightly coupled events, and blockade of calcium channels inhibits GnRH release. Thus it can be argued that the event of GnRH secretion and calcium oscillations comprise the basis for this “GnRH pulse generator”.

However, the pulsatile release of GnRH seems also to be coupled to action potentials [44, 45]. These studies show that each calcium oscillation is correlated with a burst of TTX-sensitive Na^+ -channel action potentials, and the entry of calcium through voltage-activated calcium channels. The action potentials precede calcium oscillations, no matter if the calcium oscillation is limited to one single cell or propagates further as an intercellular wave. Here again, K^+ -channel blockers caused distinct changes in amplitude or frequency of calcium oscillations.

Based on all these observations, a model for this mechanism has been proposed [46] and verified by more recent studies: in the beginning occurs an opening of voltage-gated sodium channels. Inward Na^+ -current evokes the firing of action potentials, which then leads to influx of calcium through voltage-gated calcium channels. Subsequent release of calcium from intracellular stores may also contribute to the increase in $[\text{Ca}^{2+}]_{\text{cyt}}$, but not necessarily. K^+ -channels, possibly Ca^{2+} - and voltage-activated, then open, causing a return of the membrane

potential to its resting value. The burst of action potentials is therefore ended and $[Ca^{2+}]_{cyt}$ also returns to its resting level. GT1 neurons may therefore be considered a neuronal model of a relatively pure form of electrically driven intracellular calcium signalling. In this model, the modulation of the action potential burst duration or burst frequency through the regulation of plasma membrane ion channels directly controls the amplitude or frequency of calcium oscillations in individual cells. Oscillations occur with increasing frequency at more depolarized membrane potentials but are abolished above certain threshold potentials. Neither GnRH nor GnRH antagonists had any effect on calcium oscillations, indicating that calcium oscillations were in turn not influenced by altered GnRH levels.

Another study focusing on the correlation between action potentials and calcium oscillations revealed that removal of extracellular calcium only abolished the calcium waves, but not the action currents [47]. Their results indicate that action currents are generated by sodium-channel action potentials and that these action potentials are required to produce repetitive Ca^{2+} transients through the activation of voltage-gated Ca^{2+} channels. Thus mere depolarization of the membrane seems not sufficient to cause influx of Ca^{2+} without the firing of Na^+ action potentials.

5.2 The correlation between action potentials and growth cone motility

There is evidence that electrical activity, in this case the occurrence of action potentials, can lead to suppression of neurite elongation and thus growth cone motility [48]. When action potentials were experimentally evoked, growth cone advance, and thus neurite elongation, was reversibly stopped. The findings show that the generation of action potentials is a sufficient signal to halt neurite outgrowth abruptly and reversibly. Changes in neurite outgrowth were accompanied by changes in growth cone structure, as the number of filopodia decreased continuously during electrical stimulation; advance often stopped within 15 minutes of the onset and growth cones resumed their growing morphology within 2 hours after stimulation. These results suggest that electrical activity in neural circuits may prevent further neurite outgrowth from synaptic partners.

Furthermore, it has been shown that the growth cone itself is highly sensitive to changes in the intracellular calcium level [41]. Action potentials produced a rise in intracellular calcium levels that is correlated with the inhibition of outgrowth.

Changes in intracellular calcium levels seem not to be necessary, but sufficient for a change in growth cone behavior. It has already been shown before that “if intracellular calcium falls below an optimal level, or rises significantly above it, growth cone mobility and neurite outgrowth are inhibited” [49].

5.3 Mechanosensitive ion channels

Evidence is growing that most cells, also neuronal cells, have mechanosensitive (MS) channels potentially capable of monitoring and regulating variations in cellular mechanics [50]. It has been found that their open probability depends on stress (tension) at the membrane and not, as assumed before, on the pressure gradient. In neuroblastoma cation-permeable stretch-activated channels have been discovered. MS channels seem to be ubiquitous across all cell types, with a uniform density of $\sim 1/\mu\text{m}^2$. Important particularly with regard to the GT1 cells might be the result that in cultured snail neurons the cell body seems mechanically quiescent, while the growth cones appear to be mechanically active. This indicates the possibility that channels are at least in part responsible for motility at the growth cone. It has also been demonstrated that

mechanostimulation (e.g. pulling with a pipette) induces an increase in $[Ca^{2+}]_{cyt}$ and thus an altered growth pattern.

This rise in intracellular calcium in response to mechanically applied stretch has also been verified in cultured ventricular cells [51]. Cells were exposed to either mild stretch resulting in an initially large transient increase in $[Ca^{2+}]_{cyt}$ followed by a sustained small increase over a longer period of time, or a quick stretch with higher intensity which resulted in only a large transient increase in $[Ca^{2+}]_{cyt}$. These increases were absent when Ca^{2+} was removed from the medium.

Along with these stretch experiments, which exerted active stretch on membranes or growth cones, it was also discovered that there is another form of stretching, the so-called “passive stretching” or “towing” [52]. This occurs when axons have formed a stable synaptic connection at their termini with the other neuron(s) and then increase in length coordinate with their surrounding tissue. This second phase, after the first active, growing phase, can be extensive and rapid.

5.4 Involvement of calcium channels in the growth behavior of other types of cells

There is evidence that calcium ions have crucial influence in neuroblastoma neurite extension [53]. In PC12 cells, NGF (nerve growth factor) serves in mobilisation of Ca^{2+} , which in turn causes increased adhesion and neurite extension. Also, membrane depolarization is said to lead to increased adhesion and neurite extension as well as increased influx of Ca^{2+} in these cells.

Furthermore, a rapid increase in cytosolic calcium also seems to be responsible for the spreading of human neutrophils [54]. Here, leukocytes placed on any surface attached and, accompanied by extensive changes in the cytoskeleton, spread and increased their diameter severalfold. Immediately before spreading, about a ninefold increase in cytosolic calcium level could be observed, which then returned to near-resting level during spreading. Data suggest that release from intracellular pools is responsible for the increase in calcium.

Quite recently the plasma membrane of leukocytes was successfully manipulated with optical tweezers to stimulate influx of extracellular calcium through membrane channels [55]. When a laser beam was dragged across the

membrane, this caused a significant increase in cytosolic calcium; the increase was again abolished in case of Ca^{2+} -free medium. The fact that addition of lansoprazole, which acts on calcium channels, to the medium also abolished a rise in calcium, allows the conclusion that the mechanical manipulation exerted by the laser beam does not damage the plasma membrane and therefore induces calcium influx, but stimulates membrane channel-mediated influx of extracellular calcium. The optical tweezers were in this case used to mimic the shear forces leukocytes usually experience *in vivo*.

5.5 Considerations with regard to the GT1 cells

After the initial experiments with the cell lines NG108 and PC12 showed these cells were growing in response to the laser beam, first theoretical approaches about the underlying mechanism were made [14]. It is known that the laser beam induces a dipole moment in polarizable particles, and so it could be possible that the laser beam exerts a dipole force on actin monomers in the growth cone, leading to increased influx of actin monomers to the center of the laser spot and thus biases polymerization. Enhanced growth is here interpreted as the result of increased actin polymerization. Furthermore, also human

leukocytes proved to respond with increased growth activity to the force exerted by the laser beam (unpublished data).

The question is now: how do we interpret these experiments? Do our observations point to other possibilities regarding the underlying mechanisms?

The most striking observations on the GT1's should be mentioned again at this time: first, obviously active growth cones with extended filopodia and lamellipodia changed their morphology within a short period of time towards a round, action potential-like shape. Second, the growth cone, once influenced by the laser beam, kept its original position with a remarkable reliability regardless of any attempts to stimulate growth in a certain direction by moving the laser spot. Third, in most cases, the cell body was moving backwards, even when surrounding cells were in its way.

At first glance, it might look as if the growth cone was somehow tweezed by the laser, as in optical tweezer setups, and therefore forced the cell to grow “backwards”, still allowing the actin polymerization model as explanation, which has also been proposed for the NG108 and PC12. However, the forces we use are much too small to exert tweezing on a whole growth cone or even a cell [15]. If the growth cone area were really tweezed by this small force, it also

should have been possible to hold other parts of the cell, like the dendritic tip.

This was not the case.

Then, in comparison to naturally occurring changes in morphology, determined in experiments without application of the laser, the changes we observed under the influence of the laser were about 2-3 times faster. Also, if a growth cone undergoes such a change in morphology, according to our observations it usually either retracts completely as seen in Fig 4.9, or it reextends after some time (30-60 min).

Another striking observation was shown in Fig 4.4, but occurred more often, where a varicosity moves back along the axon towards the cell body, leaving only a very faint axon behind. This occurred naturally only when a growth cone made a stable synaptic connection to another cell and “passive stretching” as described in § 5.4 took place.

Taken all the information from the previous chapters and our results together, the following model could be a possible explanation for the behavior the GT1 cells showed in our experiments:

It is known that a train of action potentials in an actively growing neuron results in the abrupt retraction of filopodia, shrinkage of lamellipodia, and termination

of neurite extension in all growth cones (see above). So it is probable that the laser somehow initiates action potentials, since we observe these changes in the growth cone. *In vivo*, action potentials occur for the very first time right after a neuron has established a synapse with its partner neuron(s). As described in [51] to [55], in our case the laser beam could exert mechanical stress on the cell membrane, leading to the opening of Na⁺- or Ca²⁺-channels and thus to either a burst of action potentials (away from the normal pulsatile routine inherent to GT1's), or induce a calcium wave due to influx of extracellular calcium. As seen before, neither of these induces growth in GT1 cells, but calcium influx stimulates spreading of leukocytes and also increased adhesion and therefore growth in PC12 cells. Thus, the underlying mechanism for growth or enhanced spreading, respectively, in NG108/PC12 and the leukocytes could also be induced membrane channel opening due to stretch on the membrane, not necessarily actin polymerization.

Another fact supporting the idea of induced action-potentials is the observed passive stretching, as the growth cone could interpret the “unusual” (not due to the pulsatile behavior) occurrence of an action potential as having established a synapse with another cell.

We can clearly calculate the intensity distribution in the laser spot along the cell membrane according to Eq. (3.1) and (3.2), but how this affects channel opening remains unclear. For several cell types and channel types it is known how the open probability P_{op} varies with different degrees of depolarization; for GT1 cells there is no information on this topic available so far. With respect to our observations, we can only say that if a depolarization is induced by the laser, it is large enough to evoke one or several action potentials.

But, as mentioned before, we are only at the beginning with optical guiding experiments on these cells, so the precise mechanism involved remains to be elucidated at the moment.

Chapter 6

Conclusions and Outlook

Overall, the experiments on the GT1 cell line showed a completely different behavior from the other neuronal cell lines before, NG108 and PC12, with the optical guidance setup. These results call into question the model of biased actin polymerization as underlying mechanism for the previous results.

However, though it is not proven in any way yet, the idea of the laser acting on membrane ion channels by stretching the membrane seems feasible, since this explanation would apply to all our observations on different cell types quite well. As already described in §5, opening of membrane channels is not linked to axonal or dendritic growth in GT1 cells, but is responsible for the induction of action potentials and calcium waves.

Then, for PC12 cells, it is known that an increased intracellular calcium concentration leads to increased adhesion and thus increased neurite extension.

Furthermore, a rise in intracellular calcium concentration immediately precedes the spreading process of human neutrophils (leukocytes). So the behavior of

these cell types also fits into the model of membrane stretching and subsequent opening of ion channels.

This is clearly only a simplified model, and in reality the problem is probably much more complex. Different cell types have different membrane structures and different types of ion channels. So it is definitely hard to predict to what extent different cell types respond to the laser and what types of ion channels could be involved.

To further investigate the possibility that the laser causes the induction of action potentials in GT1 cells, it would be interesting to record electrical activity in the influenced cell simultaneously with the help of patch-clamp. A next step could also be to monitor calcium waves by loading the cells with fluorescent markers that detect changes in calcium concentration, like fura-2. Also, to find out more about the influence of the laser on the actin distribution in GT1 cells, it seems feasible to stain the cells with common techniques and compare the actin distributions before and after the experiment.

Another approach could be to hold the membrane potential at its resting value by patch-clamping while the growth cone is under laser influence. The induction of action-potentials is then not possible, and maybe this procedure

could reveal an overwriting effect of the action potentials over possible actin polymerization and maybe even growth.

As mentioned above, many different experiments are still ahead of us to investigate the possibilities of mechanisms responsible for the behavior of the cells we observed. The unexpected results of our experiments with the GT1 cells provide a unique opportunity to come a step closer to find the precise mechanism underlying optical neuronal guiding.

Appendices

Appendix A

List of chemicals

Name	Abbr.	purpose	vendor
HAM's F12	HAM's F12	Part of cell base medium	Cellgro (Mediatech Inc.)
Dulbecco's Modified Eagle's Medium	DMEM	Part of cell base medium	ATCC
Phosphate- buffered saline	PBS	Rinsing fluid	Self-made
Dimethyl sulfoxide	DMSO	Mixed with medium for freezing	Sigma

Fetal bovine serum	FBS	Ingredient of GT1 medium	ATCC
Laminin		Enhancement of cell adhesion	Sigma
Trypsin (0.25%)-EDTA (0.1%)-sol.		Detaching of GT1-7 cells	Cellgro (Mediatech Inc.)

Table A.1: List of chemicals

Appendix B

Cell culture procedures

1. Preparation of culture medium for GT1 cells

◆ Preparation/Materials

1. 500ml DMEM
2. 500ml HAM's F12
3. 100ml FBS
4. optional 2-20ml/l penicillin-streptomycin
5. 0.22 μ m- filter
6. autoclaved 1000ml bottle for medium

◆ Method

1. Thaw FBS and optional 2-20ml/l penicillin-streptomycin solution
2. If using penicillin, take out the equivalent volume from the media (half of both)
3. Remove 50ml from original DMEM-bottle (500ml)
4. Remove 50ml from original HAM's F12-bottle (500ml)

5. Put 0.22 μ m filter on autoclaved glass bottle. Filter both media into one bottle. Remove filter
6. Add 100ml FBS (and penicillin) to media
7. Label and store at 4°C in dark

For serum-depleted medium: no addition of FBS

2. Preparation of PBS

◆ Preparation/Materials

1. Ingredients: NaCl, KCl, Na₂HPO₄, KH₂PO₄ HCl, millipore water
2. pH-indicator paper or pH-electrode

◆ Method

1. Dissolve 8g of NaCl, 0.2g of KCl, 1.44g of Na₂HPO₄ and 0.24g of KH₂PO₄ in 800ml millipore water
2. Adjust pH to 7.6 with HCl
3. Add millipore water to 1 liter
4. Autoclave and store

3. Passaging

Growing cells divide until they cover the entire surface of the flask. At this point they must be passaged (-> next cell generation), i.e. removed from the old flask and about 1/10 of them brought into a new flask to prevent cell death. This procedure has to be done every 4-5 days, depending on how dense the cells are. With GT1 cells, special attention must be paid for this procedure, since they are sensitive to sparse plating. For GT1-1, the mechanical way of spraying medium across the monolayer is usually sufficient to detach the cells; the GT1-7 however are more adherent to the substrate and require trypsination to detach them.

◆ Method for GT1-1

1. Add 10ml of medium to new flask
2. Aspirate medium off old flask
3. Spray 1-3 ml of medium over the cells to detach them. Repeat several times

4. Redistribute 1ml of cells (for GT1) in medium in the new flask
(1 in 10), label and store in incubator

◆ **Preparation/Materials for GT1-7**

1. Pre-warm 1ml trypsin and ~ 2ml PBS per flask to 37°C

◆ **Method for GT1-7 (Trypsinizing)**

1. Remove the culture medium from the flasks
2. Carefully rinse the cell monolayer with PBS; it is essential to remove all traces of serum, which contains trypsin-inhibitors
3. Add the trypsin solution to the flask and swirl gently to cover the cell monolayer completely; allow the cells to incubate for ~1 min and check for dissociation; tapping the flask may facilitate dissociation
4. Once the cells appear dislodged, add 5ml warm complete (i.e. containing serum) medium to the flask to neutralize the action of the trypsin. Waiting too long with adding growth medium may result in cell death
5. Swirl gently to disperse cells into suspension
6. Take out suspension and fill into centrifuge tube. Centrifuge at 800rpm

for 4 min

7. Aspirate medium off
8. Add 10ml new culture medium (37°C) and redistribute in cell culture flask
9. Label and store in incubator

4. Plating on experimental dish

◆ Preparation/Materials

1. Glue a new microscope cover slide on experimental dish every time with RTV 108 silicone glue
2. Clean experimental dishes thoroughly with bleach, millipore and as last step with alcohol and autoclave in a (at least 30 min) gravity cycle
3. PBS, optional 1µl/ml laminin per dish

◆ Method

1. Add 1 ml PBS to each experimental dish for cleaning

2. Aspirate PBS off
3. Optional preparation of a laminin coating:
 - a. Mix 1ml of PBS with 1 μ l/ml of laminin. Put mixture on experimental dish and incubate at 37°C for at least 1 hour
 - b. Aspirate liquid off
 - c. Wash three times with 1ml PBS to wash away excess laminin
4. Dislodge cells from flask and redistribute in experimental dish (1ml medium with cells per dish; density around 100-200 cells/ml)
5. After 1-2 days: aspirate old medium off and replace it with ~ 1ml serum-depleted medium

5. Thawing

◆ Method

1. Pipet 10ml medium into new culture flask; incubate for at least 15 minutes to avoid excessive alkalinity of the medium during recovery of the cells

2. Remove cells from frozen storage and thaw the vial by gentle agitation in a 37°C water bath. To reduce the risk of contamination, keep the O-ring and cap out of the water.
3. Remove the vial from the water bath as soon as the contents are thawed
4. Transfer the contents of the vial to the 10ml medium from the incubator, rock back and forth to assure homogenous distribution, label and store the culture in the incubator

6. Freezing

◆ Preparation/Materials

1. Prepare freezing medium: for GT1: 90% medium and 10% DMSO.
Prepare ahead of time because slightly exothermic mixing of DMSO and serum might damage cells. 15ml medium will be sufficient to freeze 6-8 flasks of cells
2. check centrifuge (balanced, enough tubes)
3. hematocytometer, cryovials, Tryphan blue (cell counting)

◆ Method

1. Deattach cells in flasks (in case of GT1-7, trypsinize like described in “Passaging”)
2. Distribute in even parts all solution containing cells in 2 centrifuge tubes. Always keep at 37°C while preparing hematocytometer and counting cells
3. Pipet 20µl solution plus cells of each centrifuge tube (gently mix right before taking out because cells settle down very fast) into two 1ml-Eppendorf tubes
4. Add 20µl Tryphan blue to each tube
5. Prepare hematocytometer and add 10µl of mixture on each side
6. Count cells according to instructions for the hematocytometer
7. Repeat counting procedure with contents of the second tube
8. Evaluate total number of cells and calculate volume of freezing medium needed to attain a final concentration of $\sim 2.5 \times 10^6$ cells/ml medium
9. Centrifuge cells plus solution in the centrifuge tubes at 800rpm for 4 minutes
10. Aspirate off medium (rather leave a little meniscus of medium in the tubes than aspirating cells off), add freezing medium and mix well

11. Aliquot into cryovials
12. Label with cell type, passage number, concentration, volume, date and initials
13. Wrap all cryovials in paper towel and aluminum foil, store in a styrofoam box and leave it for 1 hour in the 4°C refrigerator
14. Transfer to freezer (-20°C) for ~2h
15. Transfer to freezer (-80°C) for overnight
16. After having attained a slow freeze (~ 0.1°C/min) due to this procedure, the cryovials can then be stored in liquid nitrogen

Freezing cells should be done about 1 day before cells are confluent; this assures higher viability.

Appendix C

Program for avi-files

As described in §, the Neuron program can save a desired area of any size as bitmap(BMP)-file. Two separate images, one cell-image and one laser-image, will be stored as “SCell+number” and “SLaser+number”, respectively. To recapitulate the experiment and store the interesting sequence of pictures in a convenient format, the following Matlab program was developed (thanks to Artem for helping me with programming). It reads the pictures one after another, determines the position of the laser spot and places a red circle on the respective cell picture. After completing this procedure for all pictures, it composes them to one avi-file, which for example can be played with Windows Media Player or Real Player. The avi-file is constructed to play two frames per second, so two minutes in the real experiment is played in one second.

This is the Matlab script (before running the actual program, the picture sequence needs to be determined and the values “start” and “stop” (line 2 and 3) set respectively)

```
clear F;  
start=22; <- insert desired first picture  
stop=64; <- insert desired last picture  
  
for j=start:stop  
  
    laser_file_name='SLaser0';  
    cell_file_name='SCell0';  
    out_file_name='pic0'
```

```

if j>99
    filename1=strcat(laser_file_name,num2str(j),'.BMP');
    filename2=strcat(cell_file_name,num2str(j),'.BMP');
    filename3=strcat(out_file_name,num2str(j),'.BMP');
else
    if j>9
        filename1=strcat(laser_file_name,'0',num2str(j),'.BMP');
        filename2 =strcat(cell_file_name,'0',num2str(j),'.BMP');
        filename3=strcat(out_file_name,'0',num2str(j),'.BMP');
    else
        filename1=strcat(laser_file_name,'00',num2str(j),'.BMP');
        filename2=strcat(cell_file_name,'00',num2str(j),'.BMP');
        filename3=strcat(out_file_name,'00',num2str(j),'.BMP');
    end
end

A=imread(filename1,'BMP');
B=imread(filename2,'BMP');

figure(1)
imagesc(A)
av=double(mean(mean(A)));
mx=double(max(max(A)));
cutoff=(av+(mx-av)/2)
BW= A>cutoff;
figure(3)
imagesc(BW);

[labeled,numObjects] = bwlabel(BW,4);
graindata= regionprops(labeled,'basic');
allgrains= [graindata.Area];
[m i]=max(allgrains)
coord=graindata(i).Centroid

figure(4)
imagesc(B)
colormap gray

```

```
hold on
plot (coord(1),coord(2),'ro',...
      'MarkerEdgeColor','k',...
      'MarkerFaceColor','r',...
      'MarkerSize',10)

axis off

F(j-(start-1)) = getframe;

hold off
print (filename3,'-djpeg','-r100');

end

mov = avifile('example.avi','fps',2);
mov = addframe(mov,F);
mov = close(mov);
```

Appendix D

Protocol for cell culture people

1. Wash your hands with anti-bacterial soap.
2. Before entering the room, turn off the UV-light.
3. Before crossing the black line,
 - Clean your stuff from the outside (medium etc) using Kimwipes soaked with 100% bleach and put them in the pre-cleaned inner tray
 - Put on shoe-, hair-, and mouth cover
 - Wear your lab coat
 - Wear the gloves and clean them with 70% ethanol
4. Enter the main cell culture room carrying the inner waste buckets and inner tray with your stuff.
5. Wipe out the flow hood with 70% ethanol.
6. Everything you want to use under the hood should be cleaned with 70% ethanol. The microscope should be cleaned with a Kimwipe soaked with 100% ethanol. Never spray ethanol directly on the microscope!

7. After finishing your job, wipe out the hood with 70% ethanol.
8. Check the supplies (pipettes, etc.) If there is not enough for the next person, leave a note outside for the next person. Then he/she can carry these items before he/she enters.
9. Leave the main room with the waste bucket and your stuff.
10. Put your waste in the outer waste bucket and wipe out the inner waste bucket with 70% ethanol. Never take the inner waste bucket outside the room!
11. Take off lab coat, hair and mouth cover.
12. Carry out the outer waste bucket, empty it, wipe it out with 70% ethanol and put it back in the changing room.
13. Take off shoe covers.
14. Don't forget to turn the UV-light back on.

Bibliography

- [1] Ramón y Cajal (1890). A quelle époque apparaissent les expansions des cellules nerveuses de la moelle épinière du poulet. *Anat. Anz.* 5 : 609-613, 631-639
- [2] Borgens RB (1999). Electrically mediated regeneration and guidance of adult mammalian spinal axons into polymeric channels. *Neuroscience* 91 (1): 251-64
- [3] Liu S, Bodjarian N, Langlois O, Bonnard AS, Boisset N, Peulve P, Said G, Tadie M (1998). Axonal regrowth through a collagen guidance channel bridging spinal cord to the avulsed C6 roots: functional recovery in primates with brachial plexus injury. *J Neurosci Res* 51 (6): 723-734
- [4] Zeck G, Fromherz P (2001). Noninvasive neuroelectronic interfacing with synaptically connected snail neurons immobilized on a semiconductor chip. *PNAS* 98 (18): 10457-10462
- [5] Prinz A, Fromherz P (2000). Electrical synapses by guided growth of cultured neurons from the snail *Lymnaea stagnalis*. *Biol. Cybern.* 82: L1-L5
- [6] Fromherz P, Schaden H, Vetter T (1991). Guided outgrowth of leech neurons in culture. *Neuroscience Letters* 129: 77-80
- [7] Patel N, Poo MM (1982). Orientation of neurite growth by extracellular electric fields. *Journal of Neuroscience* 2 (4): 483-496
- [8] Ashkin A (1970). Acceleration and trapping of particles by radiation pressure. *Phys Rev Lett* 24: 156-159

- [9] Ashkin A, Dziedzic JM, Bjorkholm JE, Chu S (1986). Observation of a single-beam gradient force optical trap for dielectric particles. *Optics Letters* 11 (5): 288-290
- [10] Ashkin A, Dziedzic JM (1987). Optical trapping and manipulation of viruses and bacteria. *Science* 235 (4795): 1517-1520
- [11] Ashkin A, Dziedzic JM, Yamane T (1987). Optical trapping and manipulation of single cells using infrared laser beams. *Nature* 330 (24): 769-771
- [12] Ashkin A, Dziedzic JM (1989). Internal cell manipulation using infrared laser traps. *PNAS* 86: 7914-7918
- [13] Dai J, Sheetz MP (1995). Mechanical properties of neuronal growth cone membranes studied by tether formation with laser optical tweezers. *Biophys. Journal* 68: 988-996
- [14] Ehrlicher A, Betz T, Stuhmann B, Koch D, Milner V, Raizen MG, Käs J (2002). Guiding neuronal growth with light. *PNAS* 99 (25): 16024-16028
- [15] Goegler M (2002). Light-induced actin polymerization in vitro and in vivo. Master's thesis, The University of Texas at Austin, 2002
- [16] Lodish H, Berk A, Zipurski L, Matsudaira P, Baltimore D, Darnell JE Molecular Cell Biology 4th ed., Freeman and Company
- [17] Neuroscience Tutorial, Washington University School of Medicine, <http://thalamus.wustl.edu/course/>
- [18] Letourneau PC (1979). Cell-substratum adhesion of neurite growth cone, and its role in neurite elongation. *Exp. Cell Res.* 124 (1): 127-138

- [19] Bear MF, Connors BW, Paradiso MA. Neuroscience – Exploring the brain. Second Ed., Lippincott/Williams/Wilkins
- [20] Bray D (1973). Model for membrane movements in the neural growth cone. *Nature* 244: 93-95
- [21] Mellon PL, Windle JJ, Goldsmith PC, Padula CA, Roberts JL, Weiner RI (1990). Immortalization of hypothalamic GnRH neurons by genetically targeted tumorigenesis. *Neuron* 5: 1-10
- [22] Cepko CL (1989). Immortalization of neural cells via retrovirus-mediated oncogene transduction. *Annu Rev Neurosci* 12: 47-65
- [23] Liposits Z, Merchenthaler I, Wetsel WC, Reid JJ, Mellon PL, Weiner RI, Negro-Vilar A (1991). Morphological characterization of immortalized hypothalamic neurons synthesizing luteinizing hormone-releasing hormone. *Endocrinology* 129 (3): 1575-1583
- [24] Wetsel WC, Mellon PL, Weiner RI, Negro-Vilar A (1991). Metabolism of pro-luteinizing hormone-releasing hormone in immortalized hypothalamic neurons. *Endocrinology* 129 (3): 1584-1595
- [25] Nunemaker CS, DeFazio RA, Geusz ME, Herzog ED, Pitts GR, Moenter SM (2001). Long-term recordings of networks of immortalized GnRH neurons reveal episodic patterns of electrical activity. *J Neurophysiol.* 86 (1): 86-93
- [26] Martinez de la Escalera G, Choi ALH, Weiner RI (1992). Generation and synchronization of gonadotropin-releasing hormone (GnRH) pulses: intrinsic properties of the GT1-1 GnRH neuronal cell line. *PNAS* 89: 1852-1855

- [27] Krsmanovic LZ, Stojilkovic SS, Merelli F, Dufour SM, Virmani MA, Catt KJ (1992). Calcium signalling and episodic secretion of gonadotropin-releasing hormone in hypothalamic neurons. *PNAS* 89: 8462-8466
- [28] Wetsel WC, Valenca MM, Merchenthaler I, Liposits Z, Lopez FJ, Weiner RI, Mellon PL, Negro-Vilar A (1992). Intrinsic pulsatile secretory activity of immortalized luteinizing hormone-releasing hormone-secreting neurons. *PNAS* 89: 4149-4153
- [29] Bosma MM (1993). Ion channel properties and episodic activity in isolated immortalized gonadotropin-releasing hormone (GnRH) neurons. *J. Membrane Biol.* 136: 85-96
- [30] Spergel DJ, Catt KJ, Rojas E (1996). Immortalized GnRH neurons express large-conductance calcium-activated potassium channels. *Neuroendocrinology* 63: 101-111
- [31] Javors MA, King TS, Chang X, Klein NA, Schenken RS (1995). Partial characterization of K^+ -induced increase in $[Ca^{2+}]_{cyt}$ and GnRH release in GT1-7 neurons. *Brain Res.* 694: 49-54
- [32] Selmanoff M (1997). Commentary on the use of immortalized neuroendocrine cell lines for physiological research. *Endocrine* 6: 1-3
- [33] Instruction manual for HERAcell incubators, Kendro Laboratory Products GmbH, 63450 Hanau, Germany
- [34] Greene LA, Tischler AS (1976). Establishment of a noradrenergic clonal line of rat adrenal pheochromocytoma cells which respond to nerve growth factor. *PNAS* 73: 2424-2428

- [35] Hamprecht B (1977). Structural, electrophysiological, biochemical, and pharmacological properties of neuroblastoma-glioma cell hybrids in cell culture. *Int Rev Cytol* 49: 99-170
- [36] Biosafety in microbiological and biomedical laboratories. Edited by the US Department of Health and Human Services, 4th Ed., 1999
- [37] Harada Y, Toshimitsu A (1996). Radiation forces on a dielectric sphere in the Rayleigh scattering regime. *Optics Communications* 124: 529-541
- [38] Palmer KF, Williams D (1974). Optical properties of water in the near infrared. *J. Opt. Soc. Am.* 64: 1107-1110
- [39] www.mellesgriot.com
- [40] Lankford KL, Letourneau PC (1989). Evidence that calcium may control neurite outgrowth by regulating the stability of actin filaments. *Journal of Cell Biology* 109: 1229-1243
- [41] Kater SB, Mills LR (1991). Regulation of growth cone behavior by calcium. *Journal of Neuroscience* 11 (4): 891-899
- [42] Charles AC, Kodali SK, Tyndale RF (1996). Intercellular calcium waves in neurons. *Molecular and Cellular Neuroscience* 7: 337-353
- [43] Nunez L, Villalobos C, Boockfor FR, Frawley LS (2000). The relationship between pulsatile secretion and calcium dynamics in single, living gonadotropin-releasing hormone neurons. *Endocrinology* 141 (6): 2012-2017
- [44] Costantin JL, Charles AC (2001). Modulation of Ca²⁺ signaling by K⁺ channels in a hypothalamic neuronal cell line (GT1-1). *Journal of Neurophysiology* 85 (1): 295-304

- [45] Van Goor F, Krsmanovic LZ, Catt KJ, Stojilkovic SS (1999). Control of action potential-driven calcium influx in GT1 neurons by the activation status of sodium and calcium channels. *Molecular Endocrinology* 13 (4): 587-603
- [46] Charles AC, Hales TG (1995). Mechanisms of spontaneous calcium oscillations and action potentials in immortalized hypothalamic (GT1-7) neurons. *Journal of Neurophysiology* 73 (1): 56-64
- [47] Costantin JL, Charles AC (1999). Spontaneous action potentials initiate rhythmic intercellular calcium waves in immortalized hypothalamic (GT1-1) neurons. *Journal of Neurophysiology* 82 (1): 429-435
- [48] Cohan CS, Kater SB (1986). Suppression of neurite elongation and growth cone motility by electrical activity. *Science* 232 (4758): 1638-1640
- [49] Kater SB, Mattson MP, Cohan C, Connor J (1988). Calcium regulation of the neuronal growth cone. *Trends in Neuroscience* 11 (7): 315-321
- [50] Morris CE (1990). Mechanosensitive ion channels. *Journal of Membrane Biology* 113: 93-107
- [51] Tatsukawa Y, Kiyosue T, Arita M (1997). Mechanical stretch increases intracellular calcium concentration in cultured ventricular cells from neonatal rats. *Heart Vessels* 12 (3): 128-135
- [52] Bray D (1984). Axonal growth in response to experimentally applied mechanical tension. *Developmental Biology* 102: 379-389
- [53] Hinnen R, Monard D (1980). Involvement of calcium ions in neuroblastoma neurite extension. In: *Control Mechanisms in Animal Cells*, Raven Press, New York

[54] Kruskal BA, Shak S, Maxfield FR (1986). Spreading of human neutrophils is immediately preceded by a large increase in cytoplasmic free calcium. *PNAS* 83: 2919-2923

[55] Holm A, Sundqvist T, Oeberg A, Magnusson KE (1999). Mechanical manipulation of polymorphonuclear leukocyte plasma membranes with optical tweezers causes influx of extracellular calcium through membrane channels. *Medical & Biological Engineering & Computing* 37: 410-412

Vita

Katrin Schmitt was born in Emmendingen, Germany, on the 22nd of August 1979 as daughter of Ursula Schmitt and Konrad Schmitt. After attending the Grundschule Köndringen from 1986 until 1990, the Gymnasium Kenzingen from 1990 until 1992, and the Dietrich-Bonhoeffer-Gymnasium Wertheim from 1992 until 1999, she received her Abitur in 1999. In October 1999, she started her studies of physics at the Bayerische Julius-Maximilians-Universität Würzburg, Germany. There she received her Vordiplom in August 2001 and studied for one more year in Würzburg. During these three years, she was also employed on a 30h/month-basis as a teaching assistant for pupils at Studienseminar Julianum, Würzburg. Participating in the well established exchange program between the Bayerische Julius-Maximilians-Universität Würzburg and the University of Texas at Austin, she entered graduate school at the University of Texas at Austin in September 2002. She was supported by a scholarship of the Deutscher Akademischer Auslandsdienst for her study in the USA.

Permanent address: Katrin Schmitt

Faulbacher Str. 1

97906 Faulbach/ Breitenbrunn

Germany

This thesis was typeset by the author.